MADPH-03-1345
hep-ph/0309036
September 2003

Direct and Indirect Detection of Neutralino Dark Matter In Selected Supersymmetry Breaking Scenarios

Dan Hooper[1,2] and Lian-Tao Wang[2]
[1] *Denys Wilkinson Laboratory, Astrophysics Department, OX1 3RH Oxford, England, UK*
[2] *Department of Physics, University of Wisconsin, Madison, WI 53706, USA*

Abstract

Various methods of searching for supersymmetric dark matter are sensitive to WIMPs with different properties. One consequence of this is that the phenomenology of dark matter detection can vary dramatically in different supersymmetric breaking scenarios.

In this paper, we consider the sensitivities to supersymmetric dark matter of different detection methods and techniques in a wide variety of supersymmetric breaking scenarios. We discuss the ability of various astrophysical experiments, such as direct experiments, gamma-rays satellites, neutrino telescopes and positron and anti-proton cosmic ray experiments, to test various supersymmetry breaking scenarios. We also discuss what information can be revealed about supersymmetry breaking by combining results from complementary experiments. We place an emphasis on the differences between various experimental techniques.

I. INTRODUCTION

An enormous body of evidence has accumulated in the favor of cold dark matter. This body of evidence includes observations of galactic clusters and large scale structure [1], supernovae [2] and the cosmic microwave background (CMB) anisotropies [3,4]. Recently, WMAP has provided the most detailed information on the CMB to date, quoting a total matter density of $\Omega_{\rm m}h^2 = 0.135^{+0.008}_{-0.009}$ [4]. Furthermore, data from WMAP and other prior experiments indicate a considerably smaller quantity of baryonic matter [4,5]. At the 2-σ confidence level, the density of non-baryonic, and cold, dark matter is now known to be $\Omega_{\rm CDM}h^2 = 0.113^{+0.016}_{-0.018}$ [4].

A compelling candidate for the cold dark matter is naturally provided by supersymmetry [6]. In supersymmetric models which conserve R-parity [7], the lightest supersymmetric particle (LSP), is stable. Furthermore, in many supersymmetric models, the LSP is the lightest neutralino, a mixture of the superpartners of the photon, Z and neutral higgs bosons, and is electrically neutral, colorless and a viable dark matter candidate. If such an particle were in equilibrium with photons in the early universe, as the temperature decreased, a freeze-out would occur leaving a thermal relic density. The temperature at which this occurs, and the density which remains, depends on the annihilation cross section and mass of the lightest neutralino. It is natural for supersymmetry to provide a dark matter candidate with a present abundance similar to those favored by the WMAP experiment.

Many methods have been proposed to search for evidence of neutralino dark matter. In addition to accelerator searches for supersymmetry [8], direct and indirect dark matter detection experiments have been performed. Direct dark matter searches attempt to measure the recoil of dark matter particles scattering elastically off of the detector material [9,10]. Indirect dark matter searches hope to observe the products of dark matter annihilation including gamma-rays [11–15], neutrinos [16], positrons [17–19] and anti-protons [20].

Supersymmetry with low scale soft breaking has been established as an excellent candidate for physics beyond the standard model. At low energy, a usual practice in studying supersymmetry phenomenology is to parameterize the supersymmetry breaking by putting in explicit soft supersymmetry breaking terms in the effective Lagrangian. In principle, all of those terms should be derived from some supersymmetry breaking and mediation mechanism which is embedded in the fundamental theory. Therefore, supersymmetry breaking mechanisms provide the crucial link between the fundamental theory and the low energy parameters. Knowledge of supersymmetry breaking will provide us with important information about the physics at the high energy scale. We would like to extract as much information as possible about how supersymmetry is broken from our low energy experiments. Needless to say, the identity and properties of the LSP would carry invaluable information about the underlying supersymmetry breaking mechanism. In this paper, we attempt to evaluate the prospects for direct and indirect detection of neutralino dark matter in a variety of supersymmetry breaking scenarios. We find distinctive differences in the dark matter phenomenology for various breaking mechanisms. Information from cold dark matter experiments may be very useful in providing hints about which supersymmetry breaking scenario is manifest in nature.

This paper is organized as following: First we briefly review various direct and indirect

detection methods for cold dark matter. We then review the relevent information regarding the different supersymmetry breaking scenarios that we study in this paper. Finally, we present our results and comparison of different supersymmetry breaking scenarios.

II. DIRECT DETECTION

If the dark matter halo of our galaxy is made up of TeV-scale particles, then millions of such particles travel through each square meter each second in our galaxy. Despite this large rate, dark matter particles likely have very small cross sections, making observation of such particles very difficult.

Proposed as early as twenty years ago [9], numerous experiments have been developed in an effort to directly detect dark matter particles. In this paper, we will compare theoretical predictions to recent experimental results and to the reach of future efforts.

The ability of a direct detection experiment to observe a WIMP depends on that particle's elastic scattering cross section with nucleons in the detector's target medium. This quantity depends strongly on the composition of the lightest neutralino (gaugino verses higgsino) as well as the masses of the squarks mediating scattering processes.

Limits or sensitivities are most frequently shown as a elastic scattering cross section verses WIMP mass. Since the lightest neutralino is a Majorana fermion, it only has axial-vector and scalar interactions with nuclear matter. For heavy nuclei, typically $A > 20$, the scalar (or spin independent) interaction dominates. Therefore, we focus on the limits and reaches for scalar interaction cross sections. For each model, we assume the measured local dark matter density and velocity distribution [21].

There are a large number of direct detection experiments which have been developed or are planned. Currently, the strongest sensitivities have been attained by the CDMS [22], ZEPLIN-I [23], and Edelweiss [24] experiments. Additionally, the DAMA collaboration has claimed an observation of an annual modulation in their rate consistent with a ~ 50 GeV WIMP with $\sigma_{\chi N} \sim 10^{-5}$ pb [25]. The DAMA result has been highly controversial and the entire region claimed by the experiment is now excluded by other experiments.

The next round of direct experiments include CREST-II [26], CDMS (Soudan site) [27], Edelweiss II [28] and ZEPLIN-II, III, and IV [29]. These experiments will be capable of studying WIMPs with considerably lower cross sections in the relatively near future. Later, experiments such as XENON [30] or GENIUS [31] may probe even further.

III. INDIRECT DETECTION

Several different methods have been pursued to search for cold dark matter particles indirectly. In these approaches, experiments are designed to look for annihilation products from WIMP annihilations, such as neutrinos from the Sun or Earth, gamma-rays from the center of the galaxy, and positrons or anti-protons from the galactic halo.

A. Gamma-Rays From The Galactic Center

In regions where the dark matter density is very large, the annihilation rate may become large enough to provide observable fluxes of high energy gamma-rays (and also neutrinos). The spectral [32] and angular [33] features of such a source have been studied for decades. The center of our galaxy may be such a region. Satellite-based experiments, such as EGRET and GLAST, are capable of observing gamma-rays at the energies suitable for this purpose.

The rate at which neutralinos annihilate near the galactic center depends strongly on the halo profile considered. At this time, the distribution of galactic dark matter, especially near the galactic center, is not well known. The halo models commonly discussed in this debate include distributions with low density cores, high density cusps or even higher density spikes.

N-body simulations appear to predict models with cuspy distributions, such as the Navarro, Frenk and White (NFW) or Moore, *et. al.* profiles [34]. In such models, the dark matter density increases as, $\rho \propto 1/r^{\gamma}$, near the central region. γ is 1.0 in the NFW profile and 1.5 in the Moore, *et. al.* profile. Arguments have been made, however, that observations of galactic rotation curves favor flat density core profiles [35], although others claim that these observations do not preclude the presence of a cusp at the center of our galaxy [36]. In the case of a core profile, no observable gamma-ray signal would be produced in dark matter annihilations near the galactic center region.

Models with substantial central density spikes have been discussed a great deal recently [37]. It has been argued that density spikes are generated naturally as a result of adiabatic accretion of matter into the central galactic black hole. If density spikes form in the center of galaxies, it would be possible for dark matter annihilation rates to occur near the center of our galaxy which were considerably larger than those predicted for cuspy or other halo profiles.

There are two signatures for the detection of gamma-rays from the galactic center which we will consider in this paper. The first is line emission produced from the processes $\chi^0\chi^0 \rightarrow \gamma\gamma$ and $\chi^0\chi^0 \rightarrow \gamma Z$. The second is continuum emission from all gamma-ray producing processes, dominated by π^0 decay created in the fragmentation of quarks [12]. Although the continuum emission lacks the distinctive spectral features of the line emission, the number of photons produced is considerably greater. Since there is no direct coupling between the neutralino and the photon, all line producing processes must be mediated by some charged particle loop (such as SM fermions, charginos, W-bosons, etc.). Therefore, all line emission processes are necessarily loop suppressed. For all of the diagrams contributing to line emission at the one loop level, see [13]. $\gamma\gamma$ and γZ line emission will give rise to very distinct feature in the spectrum (since the end products will have a very narrow energy distribution). The position of these lines can also be used to measure the mass of the annihilating WIMP. This is probably the only way to accurately measure the WIMP's mass outside of a collider.

B. Neutrinos From The Sun

In addition to the galactic center region, high densities of dark matter may accumulate in the center of less distant objects such as the Sun and Earth. In these deep gravitational wells, the annihilation rate of WIMPs can be large, resulting in observable fluxes of annihilation products, such as neutrinos [38]. High-energy neutrino telescopes, such as AMANDA [39], ANTARES [40] or next generation IceCube [41], are designed, in part, for this task. For a review of high-energy neutrino astronomy, see Ref. [42].

The flux of neutrinos from neutralino annihilations in the Sun or Earth is a function of the annihilation cross section of the WIMP, the WIMP-nucleon elastic scattering cross section and the ratios of the various WIMP annihilation modes. For most SUSY models, the annihilation rate reaches equilibrium with the capture rate in the Sun, and the dependence on the annihilation cross section is removed. Typically the flux of neutrinos, and the associated event rate, from WIMP annihilation in the Earth is much far smaller than from the Sun, so we will consider only the rate from the Sun in this paper.

Neutrinos can be produced in neutralino annihilation by several processes including $\chi^0\chi^0 \to t\bar{t}$, $\chi^0\chi^0 \to b\bar{b}$, $\chi^0\chi^0 \to c\bar{c}$, $\chi^0\chi^0 \to ZZ$, $\chi^0\chi^0 \to W^+W^-$ and $\chi^0\chi^0 \to \tau^+\tau^-$ [43]. Neutrinos are produced directly in the decays of $\tau^\pm$'s, c and b quarks and gauge bosons, and indirectly through the decays of the b quarks and $W^\pm$ bosons created in top quark decays. The process(es) which dominates depends on the mass and composition of the lightest neutralino. In the fragmentation process, particles can lose substantial amounts of their annihilation energy before they decay and produce a neutrino. Furthermore, high-energy neutrinos can interact as they propagate through the Sun, thus degrading their flux [43,44].

C. Positrons and Anti-Protons From The Galactic Halo

Annihilating halo neutralinos can also generate positrons and anti-protons. Unlike gamma-rays or neutrinos, charged cosmic rays do not point at their sources due to galactic magnetic fields. By measuring the flux of positrons and anti-protons at Earth, it may be possible to observe signatures of annihilating neutralinos in nearby dark matter clumps.

In 1994 and 1995, the High Energy Antimatter Telescope (HEAT) observed an excess of cosmic positrons, peaking around ~ 10 GeV [45]. This result was confirmed by another HEAT flight in 2000 [46]. Although it is uncertain whether this excess is the result of dark matter annihilation, it has been shown that halo positrons could be a signature of such a process [17–19].

Using a smooth halo profile, we calculate the positron flux on Earth following the methods of [19]. This includes not only the calculation of the injection rate of positions from neutralino annihilation, but also the propagation effects such as synchrotron and inverse Compton energy losses, which are very important. We find that for a smooth halo distribution, the positron flux predicted is probably insufficient to explain the HEAT data. Any deviations from a smooth halo profile, however, enhance the positron rate, especially if clumps occur relatively nearby. We parameterize this effect with a single variable, the

positron boost factor, which is the ratio of the positron flux at Earth for a given halo profile to the positron flux for a smooth profile.

The anti-proton flux can also be calculated [20]. Anti-protons can propagate much greater distances than positrons, however, often traveling up to ten or more kiloparsecs. This requires a separate boost factor parameter for anti-protons. The most relevant measurement of the anti-proton flux comes from the 1995 and 1997 BESS (Balloon Borne Experiment with Superconducting Spectrometer) data [47]. The anti-proton flux measured by BESS is $1.27^{+0.37}_{-0.32} \times 10^{-6}\text{cm}^{-2}\text{s}^{-1}\text{sr}^{-1}\text{GeV}^{-1}$ in the range of 400 to 560 MeV.

IV. SUPERSYMMETRY BREAKING

The general framework to study the phenomenology of softly broken low energy supersymmetry is the Minimal Supersymmetric Standard Model (MSSM). The matter spectrum of the MSSM can be obtained basically by assigning a superpartner to each of the Standard Model fields. The only exception is that in the MSSM, we require two Higgs doublets.
The MSSM superpotential is given by

$$W = \epsilon_{ab}[-\hat{H}_u^a \hat{Q}_i^b Y_u^{ij} \hat{U}_j^c + \hat{H}_d^a \hat{Q}_i^b Y_d^{ij} \hat{D}_j^c + \hat{H}_d^a \hat{L}_i^b Y_e^{ij} \hat{E}_j^c - \mu \hat{H}_d^a \hat{H}_u^b], \tag{1}$$

in which $\epsilon_{ab} = -\epsilon_{ba}$ and $\epsilon_{12} = 1$, and the superfields are defined in the standard way (suppressing gauge indices):

$$\begin{aligned}
\hat{Q}_i &= (\tilde{Q}_{L_i}, Q_{L_i}) \\
\hat{U}_i^c &= (\tilde{U}_{L_i}^c, U_{L_i}^c) \\
\hat{D}_i^c &= (\tilde{D}_{L_i}^c, D_{L_i}^c) \\
\hat{L}_i &= (\tilde{E}_{L_i}, E_{L_i}) \\
\hat{E}_i^c &= (\tilde{E}_{L_i}^c, E_{L_i}^c) \\
\hat{H}_u &= (H_u, \tilde{H}_u) \\
\hat{H}_d &= (H_d, \tilde{H}_d),
\end{aligned} \tag{2}$$

with $i, j = 1 \ldots 3$ labeling family indices. The soft breaking Lagrangian, $\mathcal{L}_{soft}$, takes the form (dropping "helicity" indices):

$$\begin{aligned}
-\mathcal{L}_{soft} = & \frac{1}{2}\left[M_3 \tilde{g}\tilde{g} + M_2 \tilde{W}^a \tilde{W}^a + M_1 \tilde{B}\tilde{B}\right] \\
& + \epsilon_{ab}[-b H_d^a H_u^b - H_u^a \tilde{Q}_i^b \tilde{A}_{u_{ij}} \tilde{U}_j^c + H_d^a \tilde{Q}_i^b \tilde{A}_{d_{ij}} \tilde{D}_j^c + H_d^a \tilde{L}_i^b \tilde{A}_{e_{ij}} \tilde{E}_j^c + h.c.] \\
& + m_{H_d}^2 |H_d|^2 + m_{H_u}^2 |H_u|^2 + \tilde{Q}_i^a m_{Q_{ij}}^2 \tilde{Q}_j^{a*} \\
& + \tilde{L}_i^a m_{L_{ij}}^2 \tilde{L}_j^{a*} + \tilde{U}_i^{c*} m_{U_{ij}}^2 \tilde{U}_j^c + \tilde{D}_i^{c*} m_{D_{ij}}^2 \tilde{D}_j^c + \tilde{E}_i^{c*} m_{E_{ij}}^2 \tilde{E}_j^c.
\end{aligned} \tag{3}$$

The m^2's, usually called soft masses squared, are in general 3×3 Hermitian matrices. $\tilde{A}$ are usually called trilinears which are 3×3 general complex matrices. In many supersymmetry breaking scenarios where $\tilde{A}$ is universal, such as mSUGRA (which we will review later), it is

common to write $\tilde{A} = Y \cdot A$. M_i's are the mass terms for the superpartners of the Standard model gauge bosons, gauginos.

Notice that the MSSM by itself is not a model of supersymmetry breaking. It is a parameterization of supersymmetry breaking by including general soft breaking terms explicitly. As a result, the MSSM has a large parameter space containing 124 parameters. Most of these are soft SUSY breaking parameters related to the masses and mixings of the superpartners, which are not measured. It is impossible to scan the full parameter space of the general MSSM for phenomenological purposes. On the other hand, all of the soft parameters are presumably generated by some underlying supersymmetry breaking and mediation mechanism. Usually, such a mechanism will provide relations between the MSSM soft parameters and reduce the number of parameters significantly. The properties make it possible, after the detection of low energy supersymmetry, to distinguish different supersymmetry breaking scenarios based on experimental data. Since the LSP appears naturally in the MSSM as a natural candidate for cold dark matter, it is interesting to study the prospects for dark matter observations in different SUSY breaking scenarios.

Most of the scenarios we consider in this article fall into the general category of gravity mediated supersymmetry breaking [48]. Gravity is a natural candidate to mediate supersymmetry breaking because regardless of other details of the model, the gravitational interaction between the hidden and the observed sector exists. For some other mediation mechanism to dominate, one must suppress the contribution from gravity. For this reason, many benchmark scenarios have been constructed and studied in the gravity mediation framework. The main alternative to gravity mediation is supersymmetry breaking mediated by gauge interactions [49]. In the gauge mediation scenario, we have approximately the following relation between the soft masses and the gravitino mass

$$\frac{m_{\tilde{g}}}{m_{\texttt{soft}}} \sim \frac{1}{\alpha_a}\frac{M_S}{M_{Pl}} \ll 1, \tag{4}$$

where M_S is some typical supersymmetry breaking scale. Therefore, generically, we will have a very light gravitino as the LSP [50]. Since we focus our attention in the paper on neutralino dark matter, we will not consider gauge mediated scenarios in detail.

Before discussing the detailed study, we briefly review the different scenarios we have considered. Notice that the patterns of soft parameters resulting from different SUSY breaking scenarios are given at the input scale, which we take to be the grand unification scale. The phenomenologically interesting low energy parameters are obtained through the running of the renormalization group equations.

A. mSUGRA

The general framework to study gravity mediated supersymmetry breaking is the N=1, D=4 supergravity Lagrangian which is an effective Lagrangian after integrating out quantum gravity effects at the Planck scale. Without a specific model, general gravity mediation will not give rise to specific predictions and relations between different parameters. The most general supergravity Lagragian would contain all of the terms allowed by gauge symmetry. However, a minimal benchmark in this scenario was constructed [48] and well studied as an

example of the physics of gravity mediated supersymmetry breaking. The main ingredients of this scenario (at the supersymmetry breaking scale) are

1. Flavor diagonal:

   The left-left and right-right blocks of sfermion mass matrices are diagonal and proportional to the unit matrix. The trilinear couplings are also universal. This type of sfermion mass matrix is primarily motivated by the phenomenological consideration of satisfying flavor constraints.

2. Universality:

   All of the diagonal soft masses are assumed to have the same value, m_0. The diagonal trilinears are also assumed to be the same, with value A_0. This is a assumption motivated largely by the simplicity of the parameter space.

3. Universality of the gaugino masses, $M_{1/2}$:

   Gauge unification, in simple GUT scenarios, implies the unification of the gaugino masses. Therefore, the mSUGRA choice of gaugino mass universalilty is primarily motivated by gauge coupling unification. Notice however, the link between these two issues is not always as direct as in the simplest scenario. Hence, as with the requirement of gauge unification, we should still treat gaugino mass unification as an assumption.

Under those assumptions, the mSUGRA model contains the following set of parameters

$$m_0, \quad A_0, \quad M_{1/2}, \quad \tan\beta, \mathtt{Sign}(\mu). \tag{5}$$

In most of the parameter space of the mSUGRA model, the LSP is Bino-like (the superpartner of the hypercharge gauge boson).

We note that despite its simplicity, mSUGRA only represents a very special corner of the possible model space of supersymmetry breaking. Most of the universality assumptions may not be present in other scenarios while still satisfying the motivations of gauge unification and respecting flavor constraints.

B. Anomaly Mediated Supersymmetry Breaking

The authors of Ref. [51] pointed out an important source of supersymmetry breaking mediation in the supergravity Lagrangian due to the so-called super-conformal anomaly. It produces a elegant solution to the flavor problem due to the "UV-insensitivity" of the soft parameters in the sense that they can be expressed purely in terms of the low energy parameters such as the Yukawa couplings and gauge couplings. Reviewing the details of the origin of such a source is outside of the scope of this paper. Instead, we will focus on the characteristics of the soft spectrum as a result of anomaly mediation. The soft spectrum of the minimal anomaly mediation is [51,52]

$$M_{\lambda^a} = \frac{\beta_{g_a}}{g_a} m_{3/2},$$

$$m_{\tilde{f}}^2 = -\frac{1}{4}\left(\frac{\partial\gamma}{\partial g}\beta_g + \frac{\partial\gamma}{\partial y}\beta_y\right) m_{3/2}^2 + m_0^2,$$
$$A_y = -\frac{\beta_y}{y} m_{3/2}, \tag{6}$$

where y collectively denotes the Yukawa couplings. The β-functions and anomalous dimensions, γ, are computed in the supersymmetric limit [51,52] and, therefore, are functions of the gauge couplings and superpotential parameters. m_0 is some addition parameter outside of the AMSB scenario, not to be confused with the universal scalar mass in the SUGRA scenario. It is added by hand mainly to give rise to a non-tachyonic stau mass. In the minimal AMSB scenario, the scalar masses squared at the GUT scale are each given by:

$$m_{\tilde{S}}^2 = m_0^2 - \frac{1}{4}\left(\frac{\partial\gamma}{\partial g}\beta_g + \frac{\partial\gamma}{\partial y}\beta_y\right) m_{3/2}^2 + \text{D terms}. \tag{7}$$

However, in non-minimal scenarios, the first term may vary.

The most obvious feature of the anomaly mediation is the proportionality of the β-function to the soft parameters. Since the origin of the mediation mechanism is the superconformal anomaly, or the scale dependence of the parameters of the Lagrangian, it is not surprising to see this proportionality to the slope of the RGE running of the parameters. Notice some important features of the anomaly mediation spectrum:

1. The main phenomenological implications of this scenario are that the gaugino masses have the ratios:

$$M_1 : M_2 : M_3 = 2.8 : 1 : 7.1 \tag{8}$$

leading to the LSP being a neutral wino [52,53], which is only slightly lighter than the charged wino (by a few hundred MeV). This leads to a long lived lightest chargino with a distinctive collider signature. Notice that in the AMSB scenario, the gluino is usually quite heavy due to its large input scale value. This will in turn lead to large squark masses, since typically $m_{\tilde{q}}^2 \sim c_0 m_{\tilde{q}}^2(0) + c_3 M_3^2(0)$, where $c_0 \sim O(1)$ and $c_3 \sim 5 - 7$.

2. Unfortunately, the slepton masses squared turn out to be negative due to the fact that the pure anomaly mediation contribution to its value is negative. This is clearly unacceptable as it will lead to a charge breaking minima. This is also the reason behind the introduction of the parameter m_0 as it parameterizes additional physics which may solve this problem. However, introducing such a parameter undermines one of the main advantages of the AMSB scenario. Since there is no good reason to assume the additional physics is universal, this may reintroduce the flavor problem. Solutions to this problem have been proposed [54], for example by combining this mechanism with an anomalous $U(1)$ gauge group [55].

AMSB is a very characteristic corner of the model space of the supersymmetry breaking. It could be important if the tree level gravity mediation (which is generically one-loop order larger than the AMSB piece) is suppressed. If AMSB is indeed the dominant contributor to the SUSY breaking, the suppression of other potential contributions (which are not suppressed in a generic supergravity Lagrangian) will be an important clue to the structure of the fundamental theory.

C. Other benchmarks

Although mSUGRA and AMSB are two of the most widely studied benchmark scenarios, there are other benchmarks proposed in recent years with different motivations. Here we give a brief survey of a few of them which we will consider.

1. Focus Point

Focus point supersymmetry [56], in its simplest realization, is a special corner of the mSUGRA parameter space. In this corner, very large scalar masses are possible without violating naturalness constraints. The resulting low energy parameters have a very important feature. Namely, the soft masses squared of the Higgs boson, $m_{H_u}^2$, very important in electroweak symmetry breaking, have pseudo fixed point behavior at the electroweak scale. They can start with a wide range of input values and run to a similar negative value at the low scale. This is interesting because it indicates that, in the focus point region, electroweak symmetry breaking does not require fine-tuning in the high energy input values.

A typical feature of the focus point region is large scalar soft masses (usually $\sim$ TeV). The LSP is usually a higgsino or a mixed higgsino-gaugino. This is quite different from the other cases where the LSP has a dominant gaugino content. The main reason for a larger higgsino content is again the larger input value of the soft scalar mass. The tree level electroweak symmetry breaking condition gives

$$\frac{1}{2}m_Z^2 \sim -m_{H_u}^2 - \mu^2. \tag{9}$$

In the typical mSUGRA scenarios, $m_{H_u}^2$ is driven to some large negative value due to the RGE running. This requires a large value of μ to give the correct Z mass. However, in the focus point region, it is possible that the large input value of the scalar soft mass makes $m_{H_u}^2$ less negative. Hence, a smaller value of μ is possible, which leads to a larger higgsino content in the LSP.

2. Michigan Benchmarks

Recently, another set of benchmark models has been proposed [57]. The main motivation of these scenarios is to consider different patterns of gaugino masses (compared to the standard relation in mSUGRA, for example). By doing so, the gluino mass does not need to be quite so heavy (as implied by mSUGRA or AMSB relations). It is shown in Ref. [57] that the fine-tuning of the electroweak symmetry breaking in the MSSM is dominated by the gluino mass. Therefore, a different prediction for the gluino mass will generically offer hope of reducing fine-tuning.

Another distinctive feature of this set of benchmark models is that each of them has a motivation in string theory, rather than making arbitrary simplifying assumptions about the pattern of the soft parameters at the input scale.

Most of these proposed benchmarks fall in the category of gravity mediated supersymmetry breaking. The main feature of these constructions is the suppression of the tree level

dilaton contribution which give rise to mSUGRA-like universal input values. Therefore, they are essentially different combinations of 1-loop contributions such as anomaly mediation, threshold corrections, and Green-Schwarz counter terms. There are also two cases in which the spectrum resembles the typical gauge mediated scenario but without a light gravitino.

For more phenomenologically minded readers, the most important information is the spectrum of superpartners presented in tables 1 and 2 of Ref. [57].

3. Gaugino Mediation

Gaugino mediated supersymmetry breaking, proposed in Ref. [58], represents another class of SUSY breaking mediation motivated by the brane-world scenario. It achieves the suppression of unwanted supersymmetry breaking effects, such as the flavor violating couplings, by the separation of the observable and hidden sectors via the separation of their respective branes. In the simplest realization, it begins with a two brane set up. Most of the matter fields, in particular the chiral fermions and their superpartners, localize on one of those branes while the supersymmetry breaking sector localizes on the other. If this is the whole description, it is again similar to the anomaly mediation scenario. The new idea in this scenario is that the vector multiplet, in particular, the gauginos, are now allowed to propagate in the bulk.

The pattern of soft masses in this scenario is straight forward to describe:

1. The gauginos will have "direct" couplings to the supersymmetry breaking sector. Therefore, their soft masses are proportional to F/M, where F is supersymmetry breaking order parameter and M is some underlying fundamental scale which characterizes the coupling between gauginos and the hidden sector (since the coupling is usually of the form of a non-renormalizable term suppressed by M). With proper choices of F and M, the gaugino masses in this scenario can be chosen to be similar to any of the other supersymmetry breaking mediation scenarios.

2. The soft masses in this scenario cannot come from the direct couplings due to the separation of the two branes. On the other hand, they can be generated from the 1-loop diagrams in which a gaugino is emitted, travels through the bulk to the supersymmetry breaking brane, gets the information of SUSY breaking and then returns to join the sfermion propagator again. Generically, the soft masses are then suppressed relative to the gaugino mass by a loop factor, $m_{\tilde{f}}^2 \sim M_\lambda^2/(16\pi^2)$.

3. At low energy, soft masses and trilinear couplings generated through the RGE runnings are all proportional to the gaugino masses and are universal (since gauge coupling is flavor diagonal). Therefore, in this scenario, any flavor violating effect is again suppressed.

Notice that the soft masses for sfermions are always positive in this model since they essentially start from zero at the high scale and get positive corrections from RGE running.

In this paper, we have considered only a small sample of possible gaugino mediated models in which the features of mSUGRA are manifest while respecting the conditions of point 2 ($m_{\tilde{f}}^2 \sim M_\lambda^2/(16\pi^2)$).

V. CALCULATION OF OBSERVABLE QUANTITIES AND PARAMETER SCAN

Assuming R-parity is conserved, a large portion of the parameter space in the scenarios mentioned above can provide a neutralino which is a viable dark matter candidate. The present relic density for such a particle can be calculated by solving the Boltzman equations. This calculation is more complicated, however, if the mass of another supersymmetric particle is only slightly greater than that of the LSP. In this situation, these particles may efficiently co-annihilate[1], lowering the relic abundance of a thermal relic [59]. We have used the DARKSUSY package for our relic density calculation which includes all coannihilations with charginos and neutralinos as well as all resonances and thresholds in the cross section calculation [60]. To calculate the supersymmetric particle spectrum, we have used the packages SUSPECT [61] and FeynHiggs [62].

The thermal relic density of neutralinos can be compared to the WMAP result of $\Omega_{\rm CDM}h^2 = 0.113^{+0.016}_{-0.018}$ [4]. It is possible, however, that the present density of dark matter particles may have been produced by non-thermal mechanisms [52,63]. With this in mind, we treat the WMAP dark matter density measurement as an upper limit for the thermal relic abundance of any given WIMP. For models which predict a thermal relic density below the WMAP measurement, we assume that non-thermal mechanisms are sufficient to generate the measured dark matter density.

There can be strong constraints on supersymmetric models imposed by measurements of the $b \to s\gamma$ branching fraction [64]. In anomaly or gaugino mediated scenarios, the supersymmetric flavor problem is solved naturally and this constraint is typically not violated. In the general MSSM or mSUGRA, however, many of the models violate this bound. On the other hand, we notice that one should treat these constraints with caution since a small deviation from mSUGRA, such as a small off diagonal term in the squark mass matrix, could change significantly the prediction for $b \to s\gamma$ without effecting the dark matter phenomenology significantly.

Ref [61] also present a scenario, called the "phenomenological" MSSM, which covers a subset of the full MSSM parameter space (18 free parameters). It essentially relaxes the universality conditions in mSUGRA between the first two generations and the third, the two Higgs soft masses squared, and the three gaugino masses. All of the off diagonal entries in the sfermion mass matrices as well as the CP violating phases are still set to be zero[2]. Although this "truncated" parameterization of the MSSM is not specifically linked to any supersymmetry breaking mechanism and is not general enough to give a model independent conclusion, it is useful to illustrate what the dark matter signature may look like if the real supersymmetry breaking scenario is outside of the models we have considered. Therefore,

---

[1]Co-annihilations are annihilations between LSPs and other supersymmetric particles, such as heavier neutralinos, charginos, staus, etc.

[2]Notice that CP violating phases could have important impact on the dark matter phenomenology. For example, they could significantly change the gaugino-quark-squark coupling and thereby have a significant impact both on annihilation and elastic scattering cross sections [65].

we also include this more general scenario in our study.

At the 2001 Snowmass meeting, a set of benchmark supersymmetry scenarios were proposed [66]. These benchmarks include representative models within mSUGRA, as well as gauge and anomaly mediated models. These selected cases help to illustrate the various phenomenological features associated with different areas of the large MSSM parameter space. Although in principle they are already included in the parameter scan of mSUGRA and AMSB, it is interesting to consider them separately as representative corners of the parameter space. Therefore, we have studied the dark matter phenomenology for many of these selected benchmarks and included them in our figures.

VI. RESULTS AND DISCUSSION

A. Results For Direct Detection Experiments

The rates and sensitivities for direct detection experiments can be reliably calculated with relatively small uncertainties which result from measurements of the local dark matter density. For this reason, results from direct detection experiments are among the most useful tests of supersymmetric dark matter.

In figures 1 and 2, we show comparisons of the neutralino mass to the scalar (spin independent) neutralino-nucleon elastic scattering cross section for a variety of models. In figure 1, the lightly shaded area corresponds to a the phenomenological MSSM search described in the previous section. The darker shaded region represents those models limited to minimal supergravity (mSUGRA). For this case, we have allowed m_0, $m_{1/2}$ and A_0 to vary between 0 and 10,000 GeV. We selected $\tan\beta$ to have values in the range of 1 to 50 and have allowed μ to take on either positive or negative values. We acknowledge that 10,000 GeV is probably outside of the interesting range for $m_{1/2}$ or A_0, but we choose to allow such values in an attempt to be inclusive. Our results would vary only slightly if we were to use an upper limit of a few TeV, for example. Also shown as dark circles are the points which we consider to be gaugino mediated supersymmetry breaking models. In such models, m_0 is less than $4\pi\, m_{1/2}$. In this manifestation, gaugino mediation is a subset of mSUGRA.

For each point shown, the relic density is below the maximum value allowed by the WMAP data ($\Omega_\chi h^2 \leq 0.129$). Models that violated accelerator limits are also not shown, except for b to $s\gamma$ limits which may be violated. The experimental limits and sensitivities, shown as lines, from top to bottom (on the right) are CDMS-March 2002 (solid) [22], ZEPLIN 1-final 2002 (dashed) [23], Edelweiss-2000+2002 (dots) [24], CRESST II-projected limit (solid) [26], CDMS-projected limit (dots) [27], Edelweiss II-projected limit (dashed) [28], ZEPLIN 4-projection (solid) [29] and XENON-1 ton projected limit (dashed) [30]. Also shown, as a solid contour, is the region which the DAMA collaboration claims evidence [25]. For a summary of present limits and projections for all direct dark matter experiments, see Ref. [67].

Figure 1 indicates that very little of mSUGRA space has been effectively probed by existing direct searches. However, future experiments such as GENIUS and XENON will

have the ability to probe nearly all mSUGRA models with LSP masses below about 200 GeV.

In figure 2, again the lightly shaded area corresponds to the phenomenological MSSM. The darker shaded region shows those models limited to minimal Anomaly Mediated Supersymmetry Breaking (mAMSB) models. In such models, we allowed m_0 to vary between 0 and 10,000 GeV and the gravitino mass, $m_{3/2}$, to vary between 25,000 and 3,000,000 GeV. Again $\tan\beta$ was selected between 1 and 50 and μ is allowed to have either sign. We acknowledge that 10,000 GeV or 3,000,000 GeV are probably outside of the interesting range for m_0 or $m_{3/2}$, respectively, but we choose to allow such values in an attempt to be inclusive. Our results would vary only slightly if we were to use a smaller upper limit.

We assumed universality of the scalar masses in the minimal AMSB model. Also shown in figure 2 are black X's which represent randomly selected non-minimal AMSB models. In these models, in addition to the parameters varied in the minimal AMSB, the scalar masses squared were allowed to vary from m_0^2 at the GUT scale. Each scalar mass squared was set to m_0^2 multiplied by a factor randomly selected between 5 and -5.

Figure 2 shows that even with future experiments, AMSB scenarios are very difficult to test with direct detection methods. In non-minimal models, these prospects are slightly better. A primary reason direct detection is difficult in AMSM models is that the value of M_3 is considerably higher than M_2 or M_1, and, therefore, squark masses tend to be much larger than the LSP mass. This leads to suppression in the s-channel diagram for neutralino-quark scattering. Additionally, AMSB typically predicts a gaugino-like LSP, less favorable for direct detection than a mixed gaugino-higgsino or pure higgsino.

Figure 3, illustrating the effect of scalars in direct detection, shows the mass of the lightest neutralino versus the universal scalar mass, m_0, in the mSUGRA scenario. The darkest points are those currently excluded by either CDMS-March 2002, ZEPLIN 1-final 2002 or Edelweiss-2000+2002. The intermediate points are testable by planned experiments including CRESST II, CDMS (Soudan), Edelweiss II or ZEPLIN 4. The lightest points are beyond the sensitivity of ZEPLIN 4.

Figure 4 shows the sensitivities to direct experiments for a variety of Snowmass and Michigan benchmark scenarios. Snowmass slopes 1a, 3 and 9 and shown as lines from left to right, respectively. Snowmass point 1b, and samples of slopes 2, 4 and 5, are shown as b, 2, 4 and 5 in the figure. For the Michigan benchmark scenarios, models A through G are shown.

Along the length of each slope shown (in the Snowmass plot), the relic density is below the maximum value allowed by the WMAP data ($\Omega_\chi h^2 \leq 0.129$). However, some of the points (rather than slopes) shown produce a larger relic density.

B. Results For Gamma-Ray Experiments

In the case of a cuspy or spiked galactic halo, gamma-ray astronomy can provide a strong test of supersymmetric dark matter. For models with flat galactic cores, however, such observations are nearly impossible in planned experiments.

In figure 5, the rate of continuum gamma-rays above 1 GeV per square meter, per year of exposure, from the galactic center is shown verses neutralino mass. A smooth NFW halo

profile is assumed. If a Moore, *et. al.* model were considered, each point would produce approximately a factor of 10^3 more events; considerably more if a spiked halo model were used. As in figures 1 and 2, the lightly shaded region represents the phenomenological MSSM, the darker region corresponds to mSUGRA models, and the darker line represents the AMSB models (minimal and non-minimal). Also shown are limits from EGRET (solid) and the predicted sensitivity for the future experiment GLAST (dashed) [14]. Note that EGRET is already sensitive to some models, and GLAST will be sensitive to many models, especially for those models with a relatively light neutralino. In AMSB scenarios, the mass parameters M_1 and M_2 are proportional to their respective couplings, so the neutralino mass and annihilation cross section become correlated, leading to the single line across the figure.

Figure 6, illustrating the effect of scalars in gamma-ray production, shows the mass of the lightest neutralino versus the universal scalar mass, m_0, in the mSUGRA scenario. The darkest points are those currently excluded by EGRET assuming a smooth NFW halo profile. The intermediate points are testable by the GLAST experiment. The lightest points are beyond the sensitivity of GLAST.

Again, we also show results for Snowmass and Michigan benchmark scenarios. Figure 7 shows the sensitivities to gamma-ray experiments for these models. The models shown are the same as those shown for the direct experiments.

In figures 8 and 9, the rate of gamma-rays from the line producing processes, $\chi^0\chi^0 \to \gamma\gamma$ and $\chi\chi \to \gamma Z$, are shown [15]. The sensitivity of GLAST is shown (dashed) for comparison. Again a smooth NFW halo profile is assumed. AMSB scenarios are the best prospect for line detection, although if a more cuspy model, such as Moore, *et. al.*, were realized, even some mSUGRA models may be observable.

C. Results For Neutrino Experiments

Neutrinos from WIMP annihilation in the Sun (or Earth), like direct detection, provide a method of dark matter detection with rates and sensitivities which can be reliably calculated.

In figures 10 and 11, we show the rates in a kilometer scale neutrino telescope, such as IceCube, per year from neutralino annihilation in the Sun. The models are represented by the various types of shading as in figures 1 and 2. The sensitivity projected for the IceCube experiment (dashed) is also shown [68]. A 50 GeV muon energy threshold has been imposed.

Some models in the phenomenological MSSM with a substantial higgsino fraction can have very large scattering cross sections and, therefore, provide observable neutrino rates. On the other hand, in either mSUGRA or AMSB scenarios, few models can be probed with kilometer scale neutrino telescopes. An important exception is the foucs point region of the mSUGRA parameter space, in which the LSP also has a large higgsino component. These rates do not depend strongly on the choice of halo profile as is the case for observations of the galactic center.

Again, we also show results for Snowmass and Michigan benchmark scenarios. Figure 12 shows the sensitivities of neutrino experiments for these models. The models shown are the same as for the direct and gamma-ray experiments.

D. Results For Positron and Anti-Proton Experiments

Figure 13 compares the positron boost factor required to explain the HEAT data to the maximum anti-proton boost factor which does not violate the BESS bound. Results are shown for a variety of models and SUSY breaking scenarios. The models are represented by the various types of shading as in figure 5. It is somewhat difficult to interpret these results, however, due to large uncertainties in the galactic halo model. First, the question of how large the positron boost factor could be is a subject of some debate. It is known that on the very large scales of galaxies and clusters of galaxies, such enhancement factors can exceed $\sim 10^2$ according to simulations [69]. Perhaps boost factors significantly above this scale could be considered unrealistic.

A second uncertainty is the degree to which the positron and anti-proton boost factors could differ. A ratio of 1 to 10 between the two factors is certainly reasonable, but it is difficult to determine how much larger this ratio could be. In figure 13, lines are shown representing the cases of equal positron and anti-proton boost factors and a positron boost factor ten times the anti-proton boost factor. Perhaps models to the upper-left of this second line are less likely to be capable of explaining the observed positron excess.

Note that even for a smooth halo profile (boost factors of one), a fraction of the supersymmetry models considered produced an anti-proton flux larger than would be consistent with the BESS data.

An LSP with lesser Bino content, such as in the AMSB (wino) or focus point (higgsino) scenarios, will have a greater chance of producing the observed positron excess. Such an LSP may annihilate dominantly into W bosons (if kinematically allowed) which makes the positron spectrum considerably easier to fit. Also, not that our positron analysis is not a fit to the observed complete positron spectrum, but rather only a fit to a single point (near the observed peak), disregarding the spectral shape. We also assume the background positron flux is known [70]. A more careful analysis should be done using a χ^2 fit to the entire observed spectrum, with the normalization of the background positron flux treated as a free parameter. The result of such an analysis [18] will be that there are supersymmetric models capable of producing the excess without a prohibitively large boost factor. Our analysis presented here is qualitatively right in the sense that it compares the relative potential for producing a positron excess between different models, which is what we are focusing on here.

E. Correlations Between Different Experimental Searches and Constraints

In some cases, the neutralino characteristics which determine the observability of one detection method also play an important role for another method. It is useful to identify these features in order to discuss the prospects for neutralino dark matter detection over multiple experimental methods.

Prospects for both direct detection experiments and indirect detection experiments which rely on WIMP scattering on the Sun or Earth depend on the elastic scattering cross section of WIMPs with nucleons. For this reason, the flux of neutrinos from the Sun from neutralino annihilation is related to the event rate in direct detection experiments. Figure 14 shows the rate of muons (from charged current neutrino interactions) from neutralino annihilation in

the Sun for the phenomenological MSSM. Black points represent models which have allready been excluded by current experiments such as CDMS-March 2002 [22], ZEPLIN 1-final 2002 [23] and Edelweiss-2000+2002 [24]. Darker points represent those models which can be tested by planned experiments with a sensitivity near that of the ZEPLIN 4-projection [29]. Lighter points fall below this sensitivity.

There is a clear correlation between the sensitivities of these two types of experiments. For models with a neutralino mass substantially above the energy threshold of neutrino telescopes, the sensitivity of an experiment such as IceCube is very similar to that of next generation direct detection experiments. Given this observation, these two methods of detection will likely be capable of confirming an observation made by the other technique. Note that this relationship is not present for all SUSY breaking scenarios, however.

Several methods of indirect detection depend strongly on the neutralino-neutralino annihilation cross section. For this reason, event rates for these experiments are correlated. For example, in figure 15, we show the rate of gamma-rays above 1 GeV, per square meter, per year of exposure, from the galactic center, verses neutralino mass, as in figure 5. Particularly high neutralino annihilation cross sections will not only result in a high rate of gamma-rays, but also a high rate of other annihilation products, including anti-protons from the galactic halo. Models in the lightly shaded region do not overproduce anti-protons in the case of a smooth halo profile, as measured with the BESS experiment [47]. Models in the darker region, however, require some degree of fine tuning in the halo model, i.e. placing clumps at large distances, to accomodate this limit. The consequence of this comparison is the conclusion that for those models in which EGRET is sensitive, they are also disfavored by anti-proton measurements. If, however, a more cuspy halo model is considered, the rate from annihilations in the galactic center region will increase, although the anti-proton and positron rates, which depend primarily on the local halo characteristics, will not be significantly affected.

If constraints from the measurements of the $b \to s\gamma$ branching fraction are considered, many models in the mSUGRA scenario can be strongly disfavored. In figures 16 and 17, we show the impact of the $b \to s\gamma$ constraint on the prospects for direct detection. In figure 16, all sample points shown correspond to the phenomenological MSSM, as described earlier. Figure 17 shows sample points in the mSUGRA scenario. In each figure, lighter points do not violate the $b \to s\gamma$ constraint. Darker points do violate this constraint.

Note that those models most easily tested by direct detection experiments are more likely to violate the $b \to s\gamma$ constraint. This is especially apparent in the case of mSUGRA where, except for small pockets, the only models which do not violate $b \to s\gamma$ are beyond the sensitivities of all present and next generation direct experiments. One pocket in which this constraint is not violated, near 60-100 GeV and 10^{-8} pb, are those mSUGRA points which are gaugino mediated. Such features make scenarios such as gaugino mediation and AMSB, which do not generally violate this constraint, appear very attractive.

F. Comparison of Different Supersymmetry Breaking Scenarios

From our numerical results, we have seen that different supersymmetry breaking scenarios generically give rise to different dark matter signatures since they predict different

Model	Direct Searches	γ-G.C. Cont.	γ-G.C. Line	ν-Sun	e^+	p^+	
mSUGRA	Good	Fair	Difficult	Difficult	Less Likely	OK	
AMSB	Difficult	Good	Fair	Difficult	Likely	OK	
Mich A, B	Fair	Difficult	Difficult	Difficult	Less Likely	OK	
Mich C	Fair	Fair	Difficult	Difficult	Difficult	OK	
Mich D, E	Difficult	Good	Difficult	Difficult	Likely	Fine Tuned	
Mich F, G	Difficult	Difficult	Difficult	Difficult	Less Likley	OK	
Gaugino Mediation	Fair	Difficult	Difficult	Difficult	Less Likely	OK	
SPS 1a	Good	Fair	Difficult	Difficult	Less Likely	OK	
SPS 1b	Difficult	Difficult	Difficult	Difficult	Less Likely	OK	
SPS 2 Focus Point	Good	Fair	Difficult	Good	Likely	OK	
SPS 3	Good	Difficult	Difficult	Difficult	Less Likely	OK	
SPS 4	Good	Fair	Difficult	Difficult	Less Likely	OK	
SPS 5	Difficult	Difficult	Difficult	Difficult	Less Likely	OK	
SPS 9	Difficult	Good	Fair	Difficult	Less Likely	OK	

TABLE I. A comparison of the detection potential and consistency of different SUSY breaking models. For direct searches, continuum gamma-rays from the galactic center, line emission gamma-rays from the galatic center and neutrinos from the sun, each breaking scenario is described as "Good", "Fair" or "Difficult". These assessments reflect the likelihood of detection with a given method. For the positron column, "Likely", "Less Likely" and "Unlikely" reflect the likelihood of neutralino annihilation in the galactic halo being capable of producing the observed positron excess. Finally, the anti-proton column evaluates whether the predicted anti-proton flux is compatiable with the BESS measurement, or if a fine tuned halo distribution is needed to reconcile such a model.

LSP properties as well as different spectra for the other superpartners. We qualitatively summarize these differences in Table I.

In Table I, we list the mSUGRA and AMSB models first, as they are the best studied scenarios. We then grouped the michigan benchmarks into four groups based on the identity of the LSP. The gaugino mediation scenario and the Snowmass benchmark points are also listed. Although these points are allready covered in the scan of mSUGRA and AMSB, we find it illustrative to study these benchmarks seperately as well.

We then assign qualitative measures such as "good", "difficult", etc., to each supersymmetry breaking scenario regarding their potential to produce observable signals in a particular experiment. For the positrons column, we do not attempt to assess the liklihood of observing such a signal, but rather estimate the plausibility that the observed positron excess could be generated from WIMP annihilations for a given SUSY model. For the antiprotons column, we assess whether the SUSY model requires fine tuning of the halo profile to remain consistent with the BESS data.

Notice that mSUGRA is not a point but rather a scenario with a sizable parameter space. Therefore, the qualitative comments assigned to mSUGRA should be understood as a general assessment applied to much of the parameter space. Different corners of mSUGRA parameter space could have quite different dark matter phenomenology. The same is true for our assessment of AMSB. Notice that these comments are necessarily qualitative and are not objective measures. For a more precise assessment, see the figures we present in this paper rather than the table.

A main lesson we can take away from Table I is that even if a single experiment cannot provide a definitive answer to distinguish between different supersymmetry breaking scenarios, a combination of the results of all the experiments could be a powerful tool in this respect. For example, several scenarios in this table could produce a sizeable signal in future direct search experiments. However, a observation (or non-observation) from the neutrino signal from the Sun/Earth could favor (or disfavor) the focus point region of the parameter space. Another example is the combination of the positron signal with direct detection. As we can see from the table, AMSB, Mich D,E, and the focus point region can give rise to a sizeable positron flux. However, their direct detection rates differ quite significantly. Notice that most of the models we study will at least give rise to a potentially observable signal in some experiment, and it will be possible to evaluate these scenarios based on the experimental results.

VII. CONCLUSIONS AND OUTLOOK

The large number of experiments designed to search for supersymmetric dark matter particles are beginning to enter a very exciting phase. Direct, indirect and collider experiments are each capable of a great deal of progress in the near future.

1. Direct Searches:

   Direct searches are expected to improve their sensitivity by more than a factor of 10^3 with planned experiments such as ZEPLIN-4 [29], GENIUS [31], or a 1 ton version of XENON [30]. With such improvements, many scenarios, including much of mSUGRA,

will be probed by these experiments. AMSB scenarios are more difficult to test by direct experiments, although some models should be accessible. Gaugino mediated models may be testable in these planned experiments.

2. Neutrinos From Solar Capture:

   Indirect experiments which involve the capture of neutralinos in the center of the Sun (or Earth) depend principally on the neutralino-nucleon elastic scattering cross section for capture and, therefore, have a tendency to be sensitive to the same models as direct experiments. In fact, we have shown that for moderate or heavy neutralinos (~ 150 GeV or heavier), IceCube and ZEPLIN-4 have very similar sensitivities. The focus point region of mSUGRA is, perhaps, the best prospect for this experimental method.

3. Gamma-Rays From The Galactic Center:

   Rates for gamma-ray (as well as positron and anti-proton) experiments depend primarily on the neutralino annihilation cross section. For these methods, the galactic halo profile can be of enormous importance. Particularly, the sensitivity of gamma-ray experiments, such as EGRET or GLAST, depend critically on the halo profile. Cuspy halo profiles often provide observable gamma-ray rates in such experiments, although profiles with lower density cores generally do not. Continuum emission of gamma-rays would be most easily observed in AMSB scenarios, although the prospects are still quite good for mSUGRA models. Gaugino mediated models are somewhat more difficult. For line emission, however, gaugino mediated models provide better rates than other mSUGRA scenarios.

4. Positrons and Anti-Protons:

   Cosmic positron and anti-proton experiments do not depend strongly on the size of the cusp, but rather on the smoothness or clumpiness of dark matter in the local region, as well as the location of any nearby clumps. As was the case for gamma-ray rates, positron and anti-proton rates are largest in AMSB scenarios.

5. Flavor Constraints:

   Flavor constraints, $b \to s\gamma$ in particular, can reveal important information relevant to neutralino dark matter phenomenology. In breaking scenarios without a solution to the flavor problem, SUGRA for example, many models violate this constraint, especially those which are most easily probed by direct experiments, or indirect experiments which use WIMP capture in the Sun. Scenarios which include a solution to the flavor problem, such as AMSB, do not often have such features.

6. Correlations and Comparisons:

   By combining the results of multiple experimental techniques, characteristics of a particular supersymmetry breaking mechanism may be observed. For example, rates which depend primarily on the LSP annihilation cross section could be combined with rates which depend on the LSP-nucleon elastic scattering cross section. We find that by combining all the experimental data which can be obtained in the foreseeable future, it may be possible to actually make distinctions between a variety of SUSY breaking scenarios.

7. Other Future Prospects:

   With the current operation of the Tevatron and future running of the Large Hadron Collider (LHC), it is very likely that supersymmetry will be discovered. With measurements of the supersymmetric spectrum (or portions of it), the problem of predicting event rates for direct and indirect dark matter experiments will likely become much more simple. Additionally, astronomical measurements of the galactic halo profile will shed a great deal of light on the prospects for indirect detection. It appears that a great deal of information is beginning to converge and an answer to these questions may not be far away.

ACKNOWLEDGMENTS

We would like to thank Lars Bergstrom and Graham Kribs for insightful communications. We would also like to thank Tilman Plehn and Gordon Kane for useful comments on the draft. This research was supported in part by the U.S. Department of Energy under Grants No. DE-FG02-95ER40896 and in part by the Wisconsin Alumni Research Foundation.

REFERENCES

[1] K. Abazajian *et al.* [SDSS Collaboration], arXiv:astro-ph/0305492; K.G. Begeman, A.H. Broeils, R.H. Sanders, Mon. Not. R. Astr. Soc. **249**, 523 (1991); M. Davis, G. Efstathiou, C. S. Frenk and S. D. White, Astrophys. J. **292**, 371 (1985).

[2] S. Perlmutter *et al.* [Supernova Cosmology Project Collaboration], Astrophys. J. **517**, 565 (1999) [astro-ph/9812133].

[3] P. de Bernardis *et al.*, Nature **404**, 955 (2000) [astro-ph/0004404]; S. Hanany *et al.*, Astrophys. J. **545**, L5 (2000) [arXiv:astro-ph/0005123]; A. Balbi *et al.*, Astrophys. J. **545**, L1 (2000) [Erratum-ibid. **558**, L145 (2001)]; C. B. Netterfield *et al.* [Boomerang Collaboration], Astrophys. J. **571**, 604 (2002).

[4] C. L. Bennett *et al.*, arXiv:astro-ph/0302207.

[5] S. Burles, K. M. Nollett, J. N. Truran and M. S. Turner, Phys. Rev. Lett. **82**, 4176 (1999); M. Fukugita, C. J. Hogan and P. J. Peebles, Astrophys. J. **503**, 518 (1998); S. Burles, K.M. Nollett, J.N. Truran and M.S. Turner, Phys. Rev. Lett. **82**, 4176 (1999) astro-ph/9901157.

[6] H. Goldberg, Phys. Rev. Lett. **50**, 1419 (1983); J. Ellis, J. S. Hagelin, D. V. Nanopoulos, K. Olive and M. Srednicki, Nucl. Phys. B **238**, 453 (1984).

[7] S. Weinberg, Phys. Rev. D **26**, 287 (1982); L. J. Hall and M. Suzuki, Nucl. Phys. B **231**, 419 (1984); B. C. Allanach, A. Dedes and H. K. Dreiner, Phys. Rev. D **60**, 075014 (1999).

[8] R. Barate *et al.* [ALEPH Collaboration], Phys. Lett. B **499**, 67 (2001); G. Abbiendi *et al.* [OPAL Collaboration], Eur. Phys. J. C **14**, 51 (2000); M. Acciarri *et al.* [L3 Collaboration], Phys. Lett. B **471**, 280 (1999); A. Heister *et al.* [ALEPH Collaboration], Phys. Lett. B **526**, 206 (2002); D. Acosta *et al.* [CDF Collaboration], Phys. Rev. D **65**, 091102 (2002); F. Abe *et al.* [CDF Collaboration], Phys. Rev. D **56**, 1357 (1997); B. Abbott *et al.* [D0 Collaboration], Phys. Rev. D **60**, 031101 (1999); B. Abbott *et al.* [D0 Collaboration], Phys. Rev. D **63**, 091102 (2001); S. Abel *et al.* [SUGRA Working Group Collaboration], hep-ph/0003154.

[9] A. Drukier and L. Stodolsky, Phys. Rev. D **30**, 2295 (1984); M. W. Goodman and E. Witten, Phys. Rev. D **31**, 3059 (1985).

[10] A. Bottino, V. de Alfaro, N. Fornengo, S. Mignola and S. Scopel, Astropart. Phys. **2**, 77 (1994); H. Baer and M. Brhlik, Phys. Rev. D **57**, 567 (1998).

[11] L. Bergstrom, J. Edsjo and P. Ullio, Phys. Rev. Lett. **87**, 251301 (2001); L. Bergstrom, J. Edsjo and C. Gunnarsson, Phys. Rev. D **63**, 083515 (2001).

[12] H. U. Bengtsson, P. Salati and J. Silk, Nucl. Phys. B **346**, 129 (1990); V. Berezinsky, A. Bottino and G. Mignola, Phys. Lett. B **325**, 136 (1994) [arXiv:hep-ph/9402215].

[13] L. Bergstrom and P. Ullio, Nucl. Phys. B **504**, 27 (1997) [arXiv:hep-ph/9706232].

[14] D. Hooper and B. L. Dingus, arXiv:astro-ph/0210617.

[15] L. Bergstrom, P. Ullio and J. H. Buckley, Astropart. Phys. **9**, 137 (1998).

[16] J. Silk, K. Olive and M. Srednicki, Phys. Rev. Lett. **55**, 257 (1985); F. Halzen, T. Stelzer and M. Kamionkowski, Phys. Rev. D **45**, 4439 (1992); J. L. Feng, K. T. Matchev and F. Wilczek, Phys. Rev. D **63**, 045024 (2001); V. D. Barger, F. Halzen, D. Hooper and C. Kao, Phys. Rev. D **65**, 075022 (2002); J. L. Feng, K. T. Matchev and F. Wilczek, Phys. Rev. D **63**, 045024 (2001); V. Berezinsky, A. Bottino, J. Ellis, N. Fornengo, G. Mignola and S. Scopel, Astropart. Phys. **5**, 333 (1996) [hep-ph/9603342];

L. Bergstrom, J. Edsjo and P. Gondolo, Phys. Rev. D **55**, 1765 (1997); Phys. Rev. D **58**, 103519 (1998); L. Bergstrom, J. Edsjo and M. Kamionkowski, Astropart. Phys. **7**, 147 (1997); A. Corsetti and P. Nath, Int. J. Mod. Phys. A **15**, 905 (2000); A. E. Faraggi, K. A. Olive and M. Pospelov, Astropart. Phys. **13**, 31 (2000); J. Silk, K. Olive and M. Srednicki, Phys. Rev. Lett. **55**, 257 (1985); K. Freese, Phys. Lett. B **167**, 295 (1986); L. M. Krauss, M. Srednicki and F. Wilczek, Phys. Rev. D **33**, 2079 (1986); T. K. Gaisser, G. Steigman and S. Tilav, Phys. Rev. D **34**, 2206 (1986).

[17] E. A. Baltz, J. Edsjo, K. Freese and P. Gondolo, Phys. Rev. D **65**, 063511 (2002); G. L. Kane, L. T. Wang and J. D. Wells, Phys. Rev. D **65**, 057701 (2002); M. Kamionkowski and M. S. Turner, Phys. Rev. D **43**, 1774 (1991); E. A. Baltz, J. Edsjo, K. Freese and P. Gondolo, arXiv:astro-ph/0211239.

[18] G. L. Kane, L. T. Wang and T. T. Wang, Phys. Lett. B **536**, 263 (2002) [arXiv:hep-ph/0202156].

[19] E. A. Baltz and J. Edsjo, Phys. Rev. D **59** (1999) 023511 [arXiv:astro-ph/9808243].

[20] L. Bergstrom, J. Edsjo and P. Ullio, arXiv:astro-ph/9906034; A. Bottino, F. Donato, N. Fornengo and P. Salati, Phys. Rev. D **58**, 123503 (1998); F. Donato, N. Fornengo, D. Maurin, P. Salati and R. Taillet, arXiv:astro-ph/0306207.

[21] E. I. Gates, G. Gyuk and M. S. Turner, Astrophys. J. **449**, L123 (1995) [astro-ph/9505039]; M. Kamionkowski and A. Kinkhabwala, Phys. Rev. D **57**, 3256 (1998) [hep-ph/9710337]; G. R. Knapp et.al., Astron. J. **83**, 1585 (1978); F. J. Kerr and D. Lynden-Bell, Mon. Not. R. Astr. Soc. **221**, 1023 (1986); J. A. R. Caldwell and J. M. Coulsen, Astron. J. **93**, 1090 (1987).

[22] D. Abrams *et al.* [CDMS Collaboration], Phys. Rev. D **66**, 122003 (2002) [arXiv:astro-ph/0203500].

[23] IDM 2002, York, UK (2002).

[24] A. Benoit *et al.*, Phys. Lett. B **545**, 43 (2002) [arXiv:astro-ph/0206271].

[25] R. Bernabei *et al.* [DAMA Collaboration], Riv. Nuovo Cimento. 26, I (2003) [arXiv:astro-ph/0307403]; R. Bernabei *et al.* [DAMA Collaboration], Phys. Lett. B **480**, 23 (2000).

[26] A. Morales, TAUP99, Paris (1999).

[27] TAUP99, Paris (1999).

[28] O. Martineau, DM2002, Marina Del Ray (2000).

[29] H. Wang, DM2002, Marina Del Ray (2000).

[30] E. Aprile and C. Hailey, see Ref. [67].

[31] H. V. Klapdor-Kleingrothaus, L. Baudis, A. Dietz, G. Heusser, B. Majorovits and H. Strecker, Nucl. Instrum. Meth. A **481**, 149 (2002) [arXiv:hep-ex/0012022].

[32] M. Srednicki, S. Theissen and J. Silk, Phys. Rev. Lett. **56**, 263 (1986); S. Rudaz, Phys. Rev. Lett. **56**, 2128 (1986); L. Bergstrom and H. Snellman, Phys. Rev. **D37**, 3737 (1988); A. Bouquet, P. Salati and J. Silk, Phys. Rev. **D40**, 3168 (1989).

[33] M. S. Turner, Phys. Rev. **D34**, 1921 (1986); J. Gunn, *et al.*, Astrophys. J. **233**, 1015 (1978); F. Stecker, Astrophys. J. **223**, 1022 (1978).

[34] J. F. Navarro, C. S. Frenk and S. D. White, Astrophys. J. **462**, 563 (1996) [arXiv:astro-ph/9508025]; J. F. Navarro, C. S. Frenk and S. D. White, Astrophys. J. **490**, 493 (1997); B. Moore, S. Ghigna, F. Governato, G. Lake, T. Quinn, J. Stadel and P. Tozzi, Astrophys. J. **524**, L19 (1999).

[35] P. Salucci and A. Borriello, Mon. Not. Roy. Astron. Soc. **323**, 285 (2001) [arXiv:astro-ph/0106251]; J. J. Binney and N. W. Evans, MNRAS, 327, L27 (2001).
[36] F. C. Van Den Bosch and R. A. Swaters, [arXiv:astro-ph/0006048].
[37] G. Bertone, G. Sigl and J. Silk, from a Dark Matter Spike at the arXiv:astro-ph/0203488; astro-ph 0203488;Dark-Matter Spike at the Galactic Center?," Phys. Rev. D **64**, 043504 (2001) [arXiv:astro-ph/0101481]; P. Gondolo and J. Silk, center," Phys. Rev. Lett. **83**, 1719 (1999) [arXiv:astro-ph/9906391].
[38] J. Silk, K. Olive and M. Srednicki, Phys. Rev. Lett. **55**, 257 (1985); L. M. Krauss, K. Freese, D. N. Spergel and W. H. Press, Astrophys. J. **299**, 1001 (1985); K. Freese, Phys. Lett. B **167**, 295 (1986); L. M. Krauss, M. Srednicki and F. Wilczek, Phys. Rev. D **33**, 2079 (1986); T. Gaisser, G. Steigman and S. Tilav, Phys. Rev. D **34**, 2206 (1986).
[39] Andres, E., *et al.*, 2001, Nature 410, 441.
[40] E. Aslanides, E., *et al*, 1999, astro-ph/9907432.
[41] Ahrens, J., *et al.*, 2003, to be published in Particle Astrophysics, astro-ph/0305196.
[42] F. Halzen and D. Hooper, Rept. Prog. Phys. **65**, 1025 (2002) [arXiv:astro-ph/0204527]; J. G. Learned and K. Mannheim, Ann. Rev. Nucl. Part. Sci. **50**, 679 (2000); T. K. Gaisser, F. Halzen and T. Stanev, Phys. Rept. **258**, 173 (1995) [hep-ph/9410384].
[43] G. Jungman and M. Kamionkowski, Phys. Rev. D **51**, 328 (1995) [arXiv:hep-ph/9407351].
[44] P. Crotty, Phys. Rev. D **66**, 063504 (2002) [arXiv:hep-ph/0205116].
[45] S. W. Barwick *et al.* [HEAT Collaboration], Astrophys. J. **482**, L191 (1997) [arXiv:astro-ph/9703192].
[46] S. Coutu *et al.* [HEAT-pbar Collaboration], "Positron Measurements With the HEAT-pbar Instrument", in Proceedings of 27th ICRC (2001).
[47] S. Orito *et al.* [BESS Collaboration], Phys. Rev. Lett. **84**, 1078 (2000) [arXiv:astro-ph/9906426].
[48] H. P. Nilles, Phys. Lett. B **115**, 193 (1982); A. H. Chamseddine, R. Arnowitt and P. Nath, Phys. Rev. Lett. **49**, 970 (1982); R. Barbieri, S. Ferrara and C. A. Savoy, Phys. Lett. B **119**, 343 (1982); L. J. Hall, J. Lykken and S. Weinberg, Phys. Rev. D **27**, 2359 (1983).
[49] M. Dine and W. Fischler, Phys. Lett. B **110**, 227 (1982); C. R. Nappi and B. A. Ovrut, Phys. Lett. B **113**, 175 (1982); L. Alvarez-Gaume, M. Claudson and M. B. Wise, Nucl. Phys. B **207**, 96 (1982); M. Dine and A. E. Nelson, Phys. Rev. D **48**, 1277 (1993) [arXiv:hep-ph/9303230]; M. Dine, A. E. Nelson and Y. Shirman, Phys. Rev. D **51**, 1362 (1995) [arXiv:hep-ph/9408384]; M. Dine, A. E. Nelson, Y. Nir and Y. Shirman, Phys. Rev. D **53**, 2658 (1996) [arXiv:hep-ph/9507378]; For a review, see G. F. Giudice and R. Rattazzi, Phys. Rept. **322**, 419 (1999) [arXiv:hep-ph/9801271].
[50] S. Dimopoulos, G. F. Giudice and A. Pomarol, Phys. Lett. B **389**, 37 (1996) [arXiv:hep-ph/9607225].
[51] L. Randall and R. Sundrum, Nucl. Phys. B **557**, 79 (1999) [arXiv:hep-th/9810155]; G. F. Giudice, M. A. Luty, H. Murayama and R. Rattazzi, JHEP **9812**, 027 (1998) [arXiv:hep-ph/9810442].
[52] T. Gherghetta, G. F. Giudice and J. D. Wells, Nucl. Phys. B **559**, 27 (1999) [arXiv:hep-ph/9904378].
[53] D. Majumdar, J. Phys. G **28**, 2747 (2002) [arXiv:hep-ph/0209278]; P. Ullio, JHEP

0106, 053 (2001) [arXiv:hep-ph/0105052].

[54] A. Pomarol and R. Rattazzi, JHEP **9905**, 013 (1999) [arXiv:hep-ph/9903448]; N. Arkani-Hamed, D. E. Kaplan, H. Murayama and Y. Nomura, JHEP **0102**, 041 (2001) [arXiv:hep-ph/0012103]; Z. Chacko, M. A. Luty, I. Maksymyk and E. Ponton, JHEP **0004**, 001 (2000) [arXiv:hep-ph/9905390]; E. Katz, Y. Shadmi and Y. Shirman, JHEP **9908**, 015 (1999) [arXiv:hep-ph/9906296]; D. E. Kaplan and G. D. Kribs, JHEP **0009**, 048 (2000), [arXiv:hep-ph/0009195].

[55] I. Jack and D. R. Jones, Phys. Lett. B **482**, 167 (2000) [arXiv:hep-ph/0003081]; I. Jack, D. R. Jones and R. Wild, Phys. Lett. B **535**, 193 (2002) [arXiv:hep-ph/0202101]; B. Murakami and J. D. Wells, arXiv:hep-ph/0302209.

[56] M. Drees and S. P. Martin, arXiv:hep-ph/9504324; J. L. Feng, K. T. Matchev and T. Moroi, Phys. Rev. Lett. **84**, 2322 (2000) [arXiv:hep-ph/9908309]; J. L. Feng, K. T. Matchev and T. Moroi, Phys. Rev. D **61**, 075005 (2000) [arXiv:hep-ph/9909334]; J. L. Feng, K. T. Matchev and F. Wilczek, Phys. Lett. B **482**, 388 (2000) [arXiv:hep-ph/0004043].

[57] G. L. Kane, J. Lykken, S. Mrenna, B. D. Nelson, L. T. Wang and T. T. Wang, Phys. Rev. D **67**, 045008 (2003) [arXiv:hep-ph/0209061].

[58] D. E. Kaplan, G. D. Kribs and M. Schmaltz, Phys. Rev. D **62**, 035010 (2000) [arXiv:hep-ph/9911293]; Z. Chacko, M. A. Luty, A. E. Nelson and E. Ponton, JHEP **0001**, 003 (2000) [arXiv:hep-ph/9911323].

[59] C. Boehm, A. Djouadi and M. Drees, Phys. Rev. D **62**, 035012 (2000); J. R. Ellis, K. A. Olive and Y. Santoso, arXiv:hep-ph/0112113; S. Mizuta and M. Yamaguchi, Phys. Lett. B **298**, 120 (1993); J. Edsjo and P. Gondolo, Phys. Rev. D **56**, 1879 (1997); J. R. Ellis, T. Falk and K. A. Olive, Phys. Lett. B **444**, 367 (1998); J. R. Ellis, T. Falk, K. A. Olive and M. Srednicki, Astropart. Phys. **13**, 181 (2000) [Erratum-ibid. **15**, 413 (2001)].

[60] P. Gondolo, J. Edsjo, L. Bergstrom, P. Ullio and E. A. Baltz, arXiv:astro-ph/0012234; http://www.physto.se∼edsjo/darksusy/.

[61] A. Djouadi, J. L. Kneur and G. Moultaka, arXiv:hep-ph/0211331.

[62] S. Heinemeyer, W. Hollik and G. Weiglein, Comput. Phys. Commun. **124**, 76 (2000) [arXiv:hep-ph/9812320].

[63] R. Jeannerot, X. Zhang and R. H. Brandenberger, JHEP **9912**, 003 (1999) [arXiv:hep-ph/9901357]; R. Kallosh, L. Kofman, A. D. Linde and A. Van Proeyen, Phys. Rev. D **61**, 103503 (2000) [arXiv:hep-th/9907124]; G. F. Giudice, I. Tkachev and A. Riotto, JHEP **9908**, 009 (1999) [arXiv:hep-ph/9907510]; G. F. Giudice, A. Riotto and I. Tkachev, JHEP **9911**, 036 (1999) [arXiv:hep-ph/9911302]; T. Moroi and L. Randall, Nucl. Phys. B **570**, 455 (2000) [arXiv:hep-ph/9906527].

[64] M. S. Alam *et al.* [CLEO Collaboration], Phys. Rev. Lett. **74**, 2885 (1995); K. Abe *et al.* [Belle Collaboration], arXiv:hep-ex/0107065; L. Lista [BABAR Collaboration], arXiv:hep-ex/0110010; B. Aubert *et al.* [BABAR Collaboration], arXiv:hep-ex/0207074;

[65] M. Brhlik, D. J. Chung and G. L. Kane, Int. J. Mod. Phys. D **10**, 367 (2001) [arXiv:hep-ph/0005158].

[66] B. C. Allanach *et al.*, in *Proc. of the APS/DPF/DPB Summer Study on the Future of Particle Physics (Snowmass 2001)* ed. N. Graf, Eur. Phys. J. C **25**, 113 (2002) [eConf **C010630**, P125 (2001)] [arXiv:hep-ph/0202233].

[67] http://dmtools.berkeley.edu/limitplots/.

[68] J. Edsjo, arXiv:astro-ph/0211354.
[69] B. Moore, T. Quinn, F. Governato, J. Stadel and G. Lake, Mon. Not. Roy. Astron. Soc. **310**, 1147 (1999) [arXiv:astro-ph/9903164]; A. A. Klypin, A. V. Kravtsov, O. Valenzuela and F. Prada, Astrophys. J. **522**, 82 (1999) [arXiv:astro-ph/9901240].
[70] I. V. Moskalenko and A. W. Strong, Astrophys. J. **493**, 694 (1998) [arXiv:astro-ph/9710124].

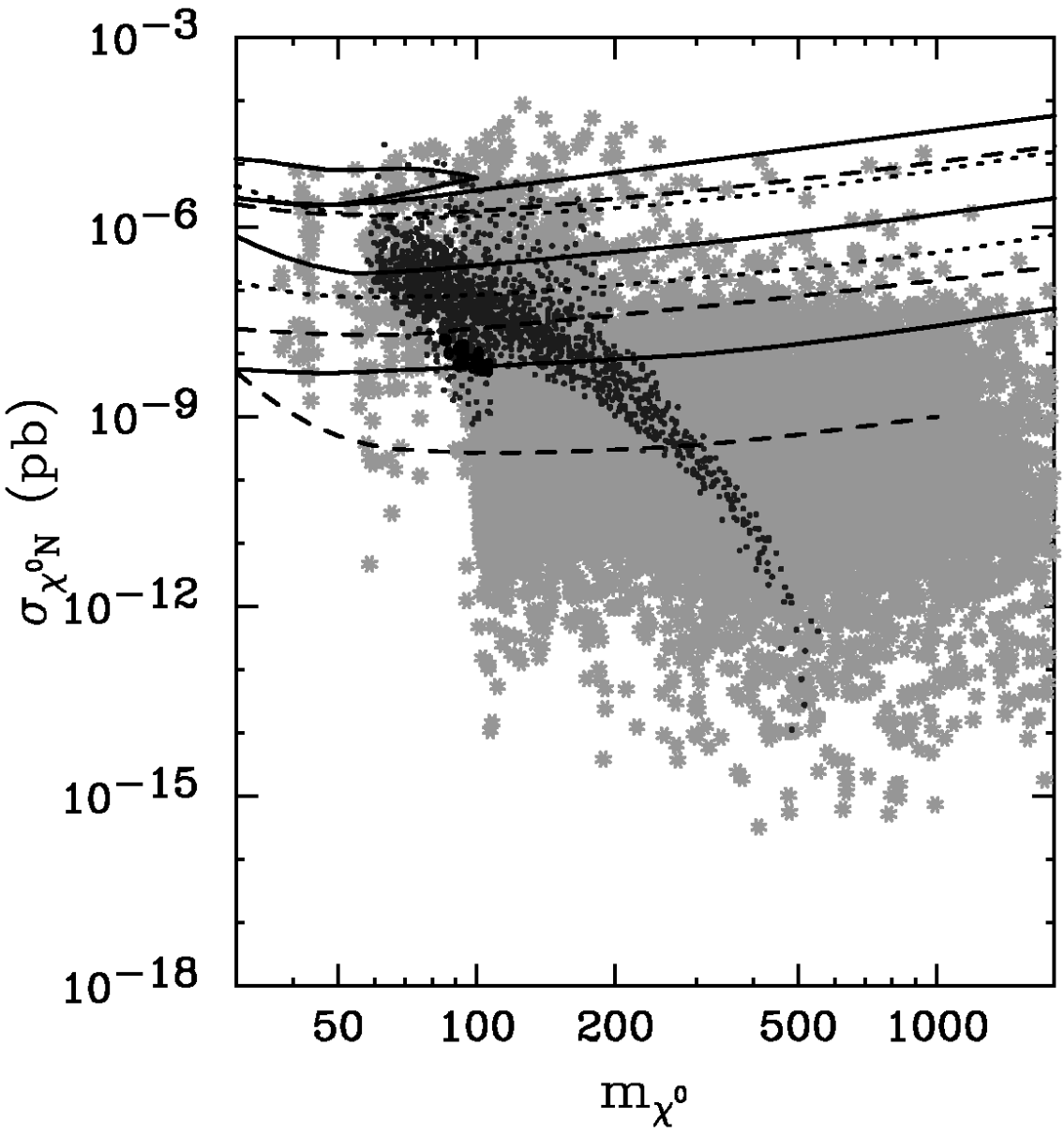

FIG. 1. The scalar (spin-independent) neutralino-nucleon elastic scattering cross section verses neutralino mass. Each point corresponds to a theoretical prediction for a specific SUSY model. The light shaded area corresponds to a general or phenomenological MSSM model. The darker colored region are those models limited to the constrained MSSM (mSUGRA). Also shown as dark circles are the points which we describe as gaugino mediated supersymmetry breaking models. See the text for more details. For each point shown, the relic density is below the maximum value allowed by the WMAP data ($\Omega_\chi h^2 \leq 0.129$). Models that violate accelerator limits are not shown, except for b to $s\gamma$ limits which will be discussed later. The experimental limits and sensitivities, shown as lines, from top to bottom (on the right) are CDMS-March 2002 (solid) [22], ZEPLIN 1-final 2002 (dashed) [23], Edelweiss-2000+2002 (dots) [24], CRESST II-projected limit (solid) [26], CDMS-projected limit (dashed) [27], Edelweiss II-projected limit (dots) [28], ZEPLIN 4-projection (solid) [29] and XENON-1 ton, projected limit (dashed) [30]. Also shown, as a solid contour, is the region which the DAMA collaboration claims discovery [25]. For a summary of present limits and projections for all direct dark matter experiments, see Ref. [67].

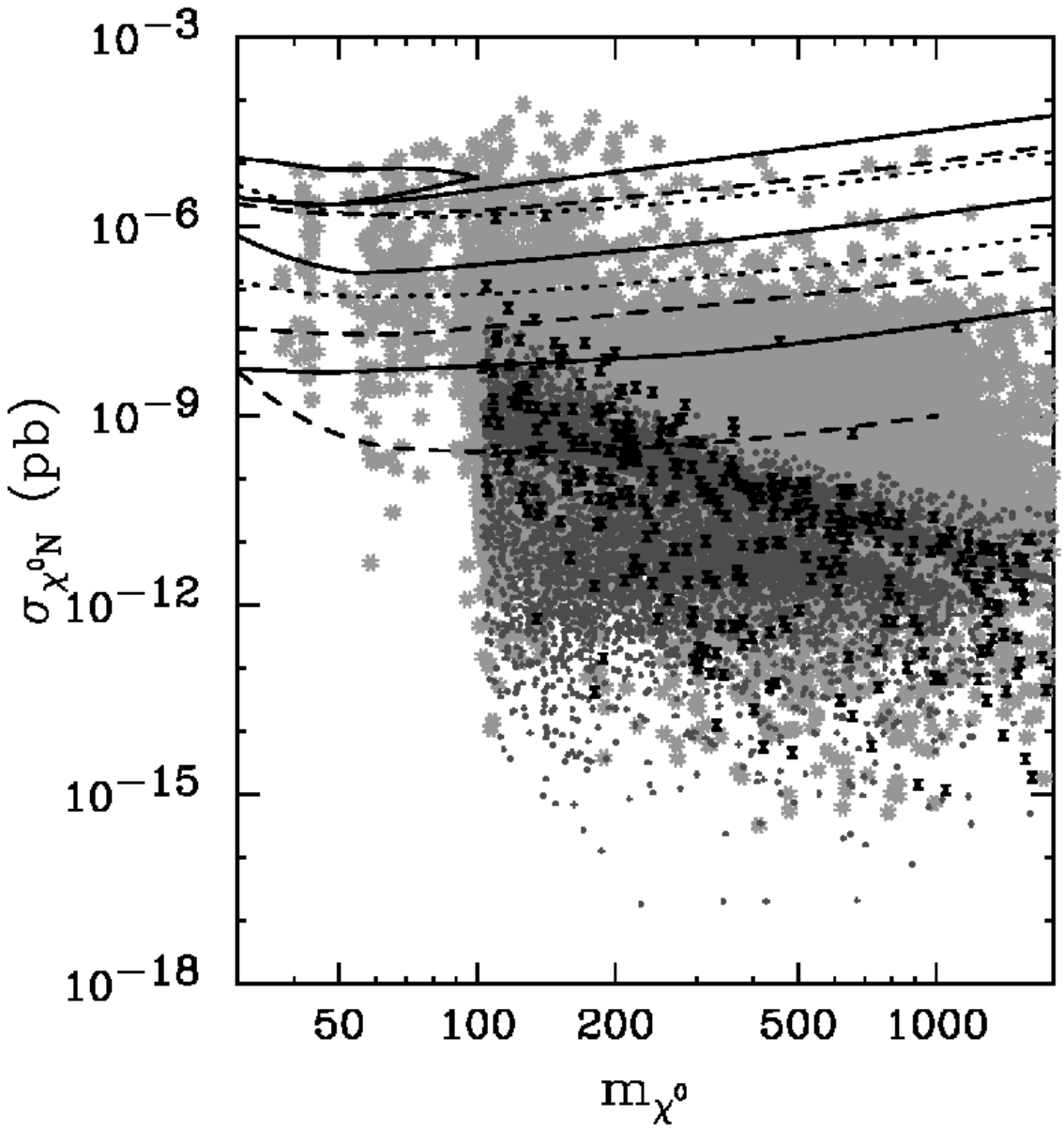

FIG. 2. The scalar (spin-independent) neutralino-nucleon elastic scattering cross section verses neutralino mass. Each point corresponds to a theoretical prediction for a specific SUSY model. The light shaded area corresponds to a general or phenomenological MSSM model. The darker shaded region shows those models limited to minimal Anomaly Mediated Supersymmetry Breaking (mAMSB) models. Also shown are black X's which represent non-minimal AMSB models. See the text for more details. For each point shown, the relic density is below the maximum value allowed by the WMAP data ($\Omega_\chi h^2 \leq 0.129$). Models that violate accelerator limits are also not shown, except for b to $s\gamma$ limits which will be discussed later. The experimental limits and sensitivities, shown as lines, from top to bottom (on the right) are CDMS-March 2002 (solid) [22], ZEPLIN 1-final 2002 (dashed) [23], Edelweiss-2000+2002 (dots) [24], CRESST II-projected limit (solid) [26], CDMS-projected limit (dashed) [27], Edelweiss II-projected limit (dots) [28], ZEPLIN 4-projection (solid) [29] and XENON-1 ton, projected limit (dashed) [30]. Also shown, as a solid contour, is the region which the DAMA collaboration claims discovery [25]. For a summary of present limits and projections for all direct dark matter experiments, see Ref. [67].

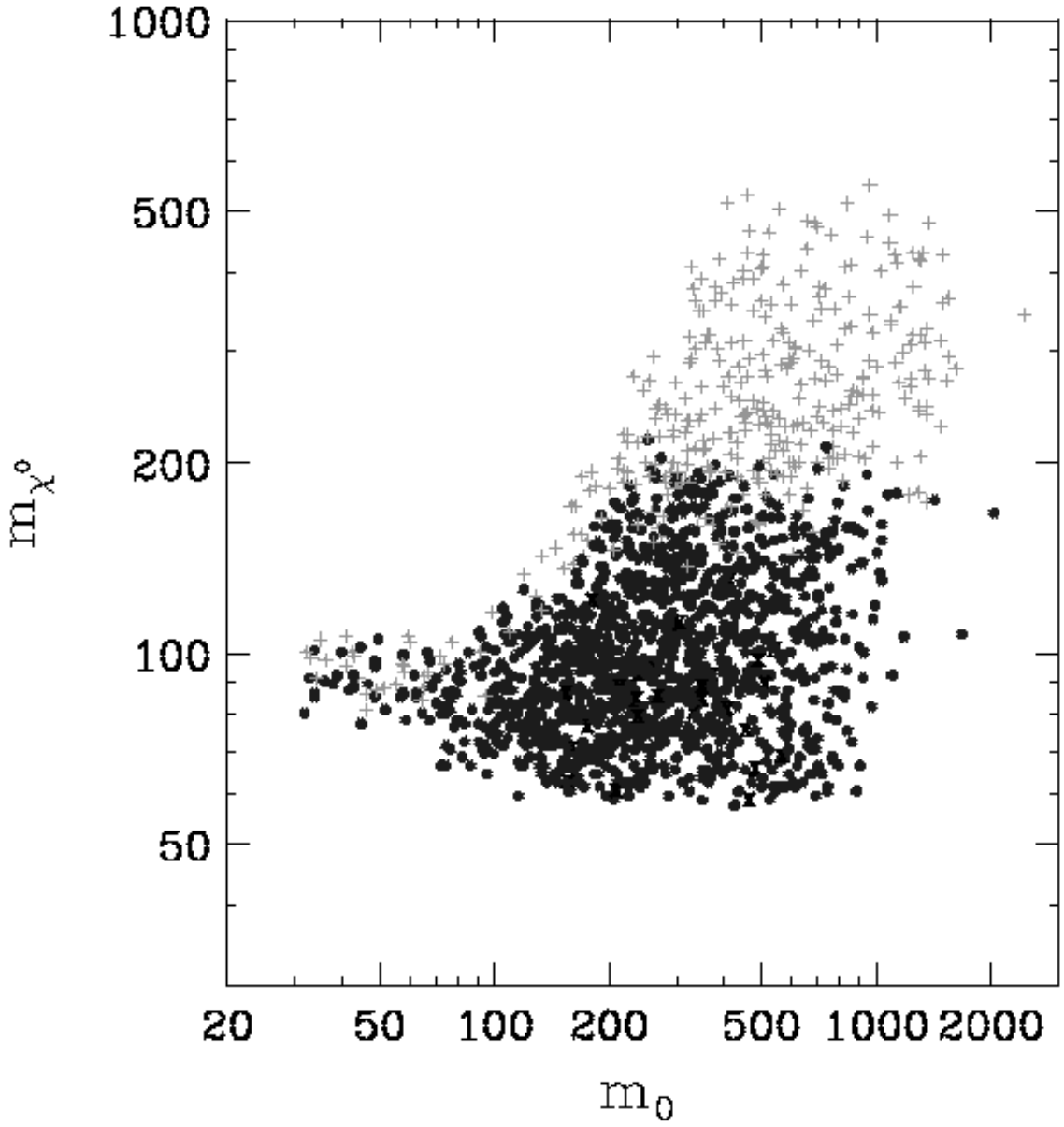

FIG. 3. The mass of the lightest neutralino versus the universal scalar mass, m_0, in the mSUGRA scenario. The darkest points are those currently excluded by one or more of CDMS-March 2002, ZEPLIN 1-final 2002 or Edelweiss-2000+2002. The intermediate points are testable by planned experiments including CRESST II, CDMS (Soudan), Edelweiss II or ZEPLIN 4. The lightest points are beyond the sensitivity of ZEPLIN 4. The models shown meet the requirements of the previous figures.

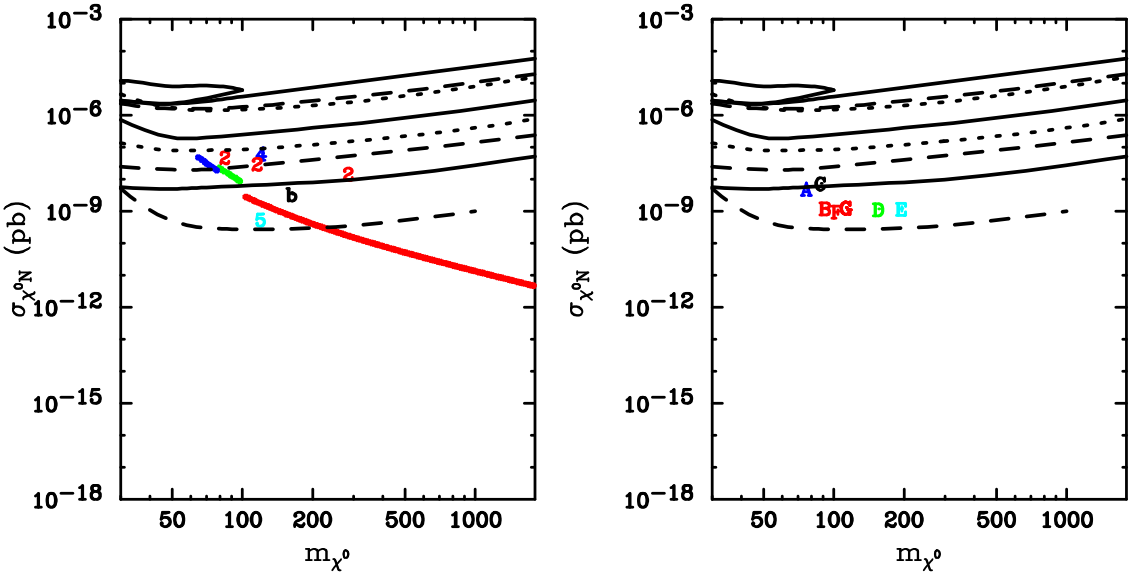

FIG. 4. The scalar (spin-independent) neutralino-nucleon elastic scattering cross section verses neutralino mass. Each point corresponds to a theoretical prediction for a specific Snowmass (left frame) or Michigan (right frame) benchmark model. In the left frame, Snowmass slopes 1a, 3 and 9 are shown as lines from left to right, respectively. Snowmass points 1b, and samples of 2, 4 and 5 are shown as B, 2, 4 and 5 in the figure. In the right frame, Michigan benchmark models A through G are shown. See the text for more details. Along the length of each Snowmass slope shown, the relic density is below the maximum value allowed by the WMAP data ($\Omega_\chi h^2 \leq 0.129$). However, some of the points (rather than slopes) shown produce a larger relic density. The experimental limits and sensitivities, shown as lines, from top to bottom (on the right) are CDMS-March 2002 (solid) [22], ZEPLIN 1-final 2002 (dashed) [23], Edelweiss-2000+2002 (dots) [24], CRESST II-projected limit (solid) [26], CDMS-projected limit (dashed) [27], Edelweiss II-projected limit (dots) [28], ZEPLIN 4-projection (solid) [29] and XENON-1 ton, projected limit (dashed) [30]. Also shown, as a solid contour, is the region which the DAMA collaboration claims discovery [25]. For a summary of present limits and projections for all direct dark matter experiments, see Ref. [67].

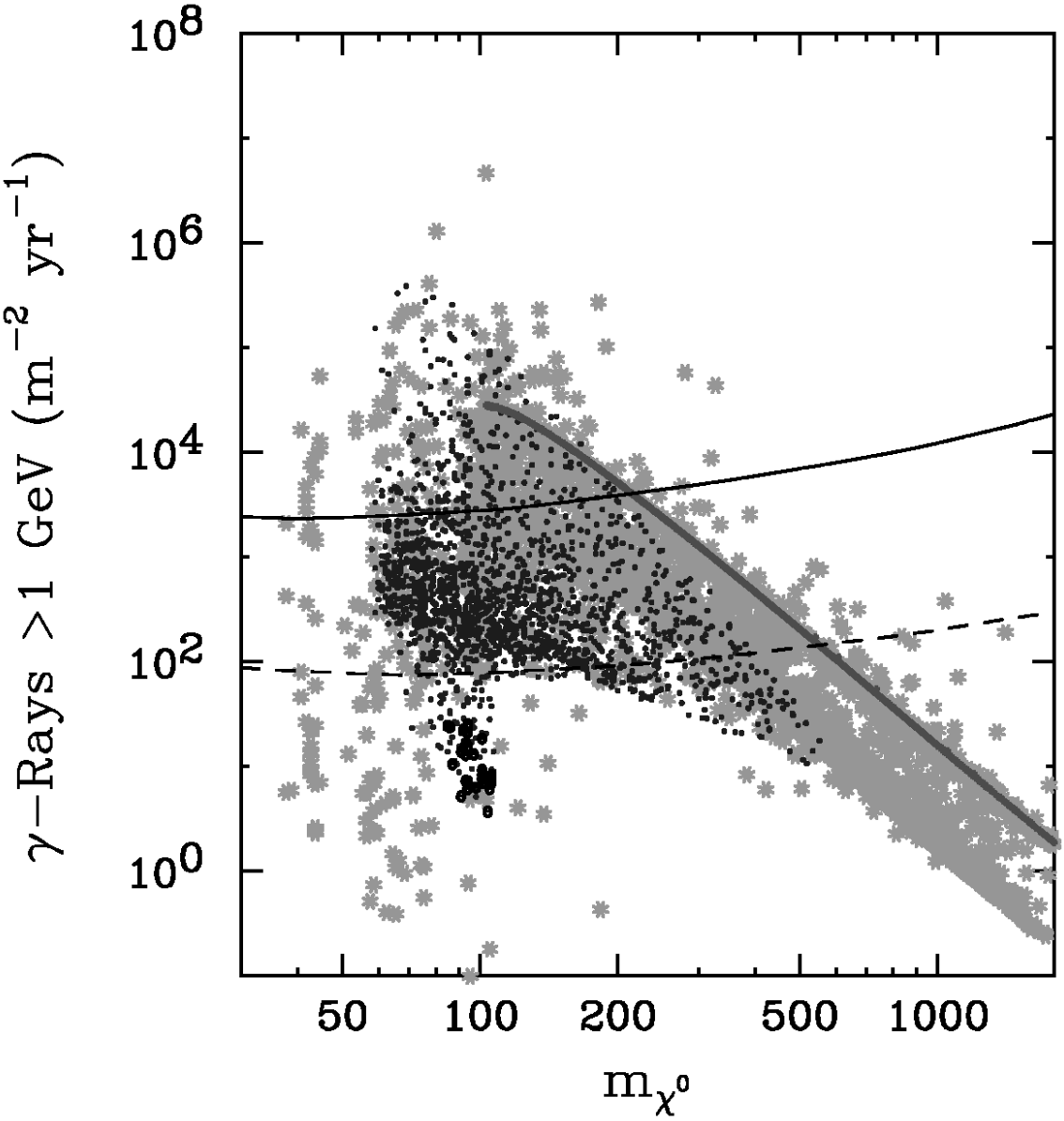

FIG. 5. The rate of continuum gamma-rays above 1 GeV per square meter, per year of exposure, from the galactic center, verses neutralino mass. A smooth NFW halo profile is assumed. If a Moore, *et. al.* model were considered, each point would produce approximately a factor of 10^3 more events. As in figures 1 and 2, the lightly shaded region is for the general or phenomenological MSSM, the darker region corresponds to mSUGRA models, the shaded line represents AMSB models (minimal and non-minimal) and black circles indicate gaugino mediated models. For each point shown, the relic density is below the maximum value allowed by the WMAP data ($\Omega_\chi h^2 \leq 0.129$). Models that violate accelerator limits are also not shown, except for b to $s\gamma$ limits which will be discussed later. See the text for more details. Also shown are limits from EGRET (solid) and the predicted sensitivity for the future experiment GLAST (dashed) [14]. Note that EGRET is already sensitive to some models, and GLAST will be sentivity to many models, especially for those models with a light neutralino. In AMSB scenarios, the mass parameters M_1 and M_2 are proportional to their respective couplings, so the neutralino mass and annihilation cross section become correlated, leading to the single line across the figure.

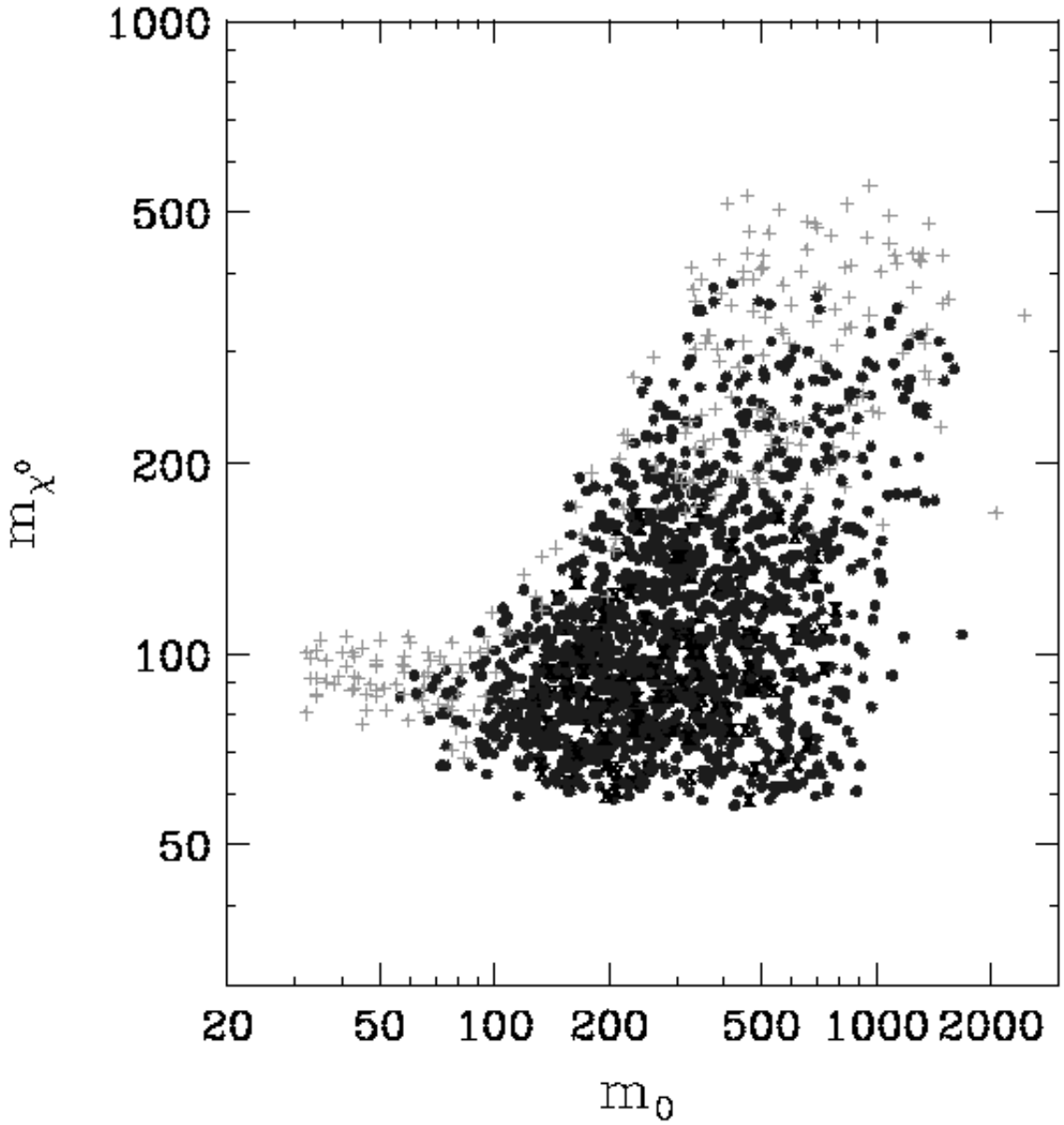

FIG. 6. The mass of the lightest neutralino versus the universal scalar mass, m_0, in the mSUGRA scenario. The darkest points are those currently excluded by EGRET assuming a smooth NFW halo profile. The intermediate points are testable by the GLAST experiment. The lightest points are beyond the sensitivity of GLAST. The models shown meet the requirements of the previous figure.

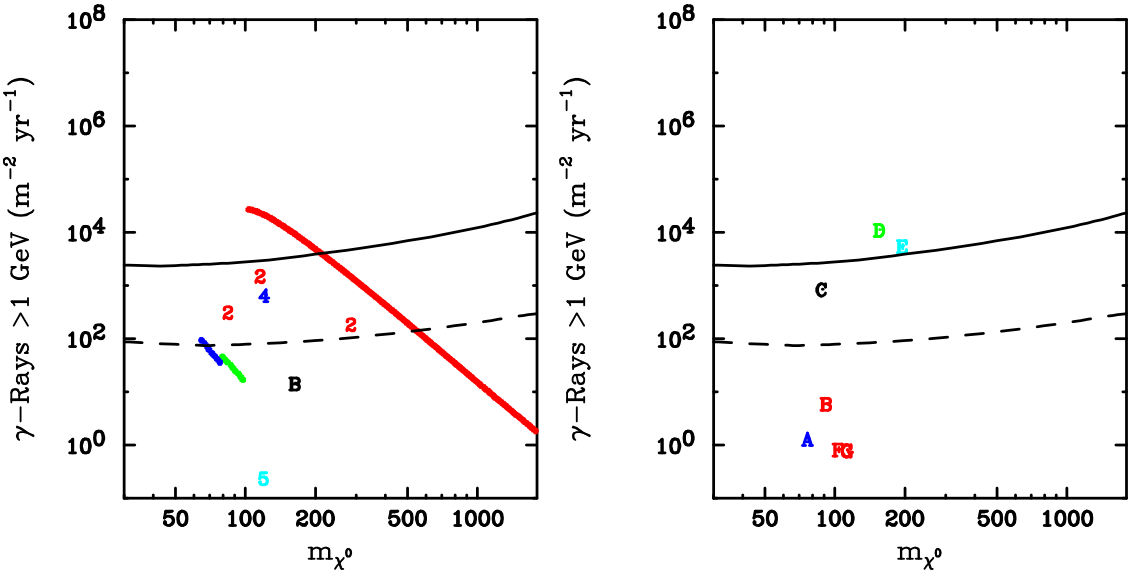

FIG. 7. The rate of continuum gamma-rays above 1 GeV per square meter, per year of exposure, from the galactic center, verses neutralino mass. A smooth NFW halo profile is assumed. If a Moore, *et. al.* model were considered, each point would produce approximately a factor of 10^3 more events. In the left frame, Snowmass slopes 1a, 3 and 9 are shown as lines from left to right, respectively. Snowmass points 1b, and samples of 2, 4 and 5 are shown as B, 2, 4 and 5 in the figure. In the right frame, each point corresponds to a theoretical prediction for a specific Michigan benchmark model. Models A through G are shown. See the text for more details. Along the length of each slope shown, the relic density is below the maximum value allowed by the WMAP data ($\Omega_\chi h^2 \leq 0.129$). However, some of the points (rather than slopes) shown produce a larger relic density. Also shown are limits from EGRET (solid) and predicted sensitivity for the future experiment GLAST (dashed) [14].

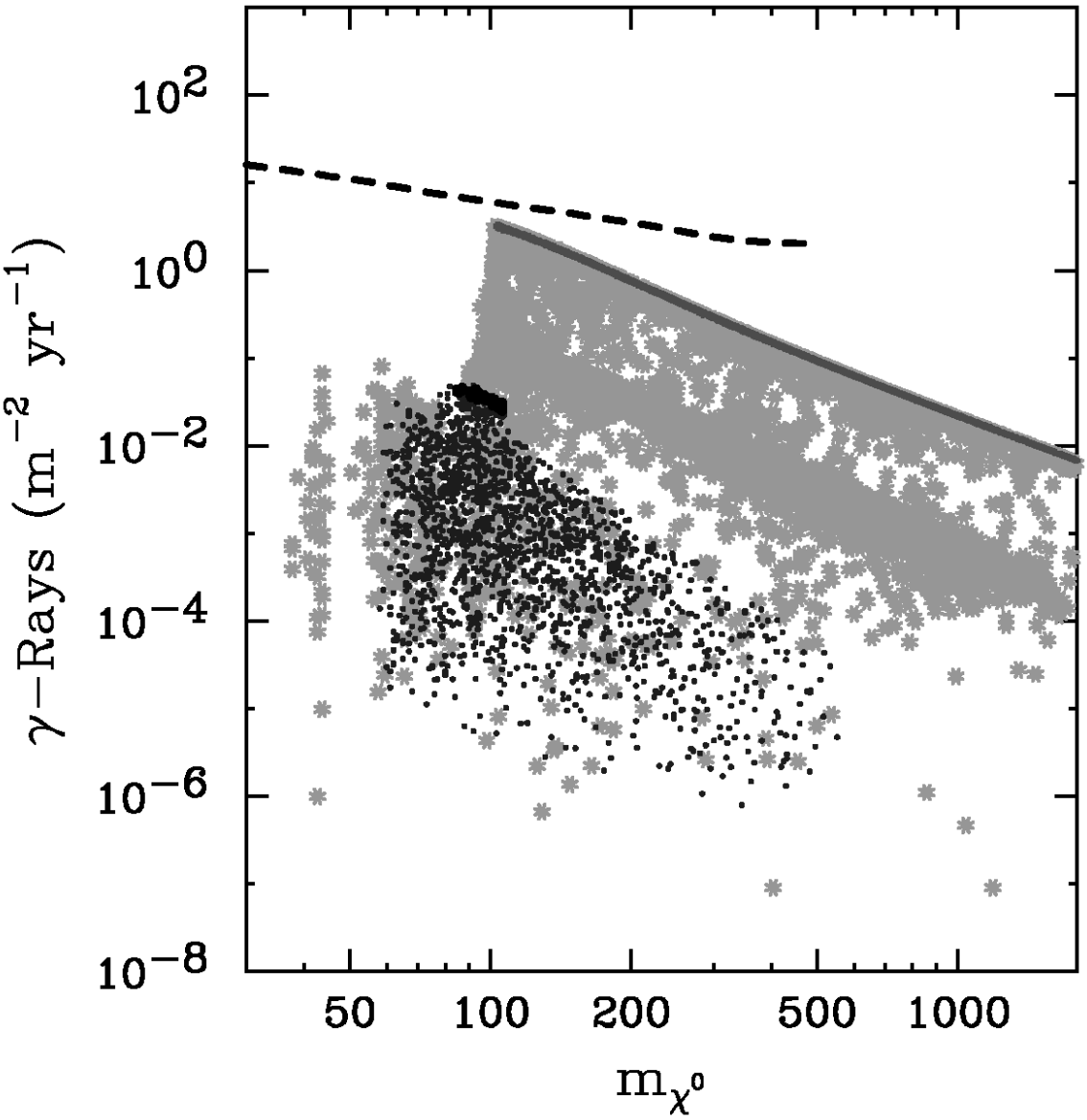

FIG. 8. The rate of gamma-rays from the process $\chi^0\chi^0 \to \gamma\gamma$ per square meter, per year of exposure, from the galactic center, verses neutralino mass. A smooth NFW halo profile is assumed. If a Moore, *et. al.* model were considered, each point would produce approximately a factor of 10^3 more events. As in figures 1 and 2, the lightly shaded region is for the general or phenomenological MSSM, the darker region corresponds to mSUGRA models, the shaded line represents AMSB models (minimal and non-minimal) and black circles indicate gaugino mediated models. For each point shown, the relic density is below the maximum value allowed by the WMAP data ($\Omega_\chi h^2 \leq 0.129$). Models that violate accelerator limits are also not shown, except for b to $s\gamma$ limits which will be discussed later. See the text for more details. Also shown is the predicted sensitivity for the future experiment GLAST (dashed) [15]. In AMSB scenarios, the mass parameters M_1 and M_2 are proportional to their respective couplings, so the neutralino mass and annihilation cross section become correlated, leading to the single line across the figure.

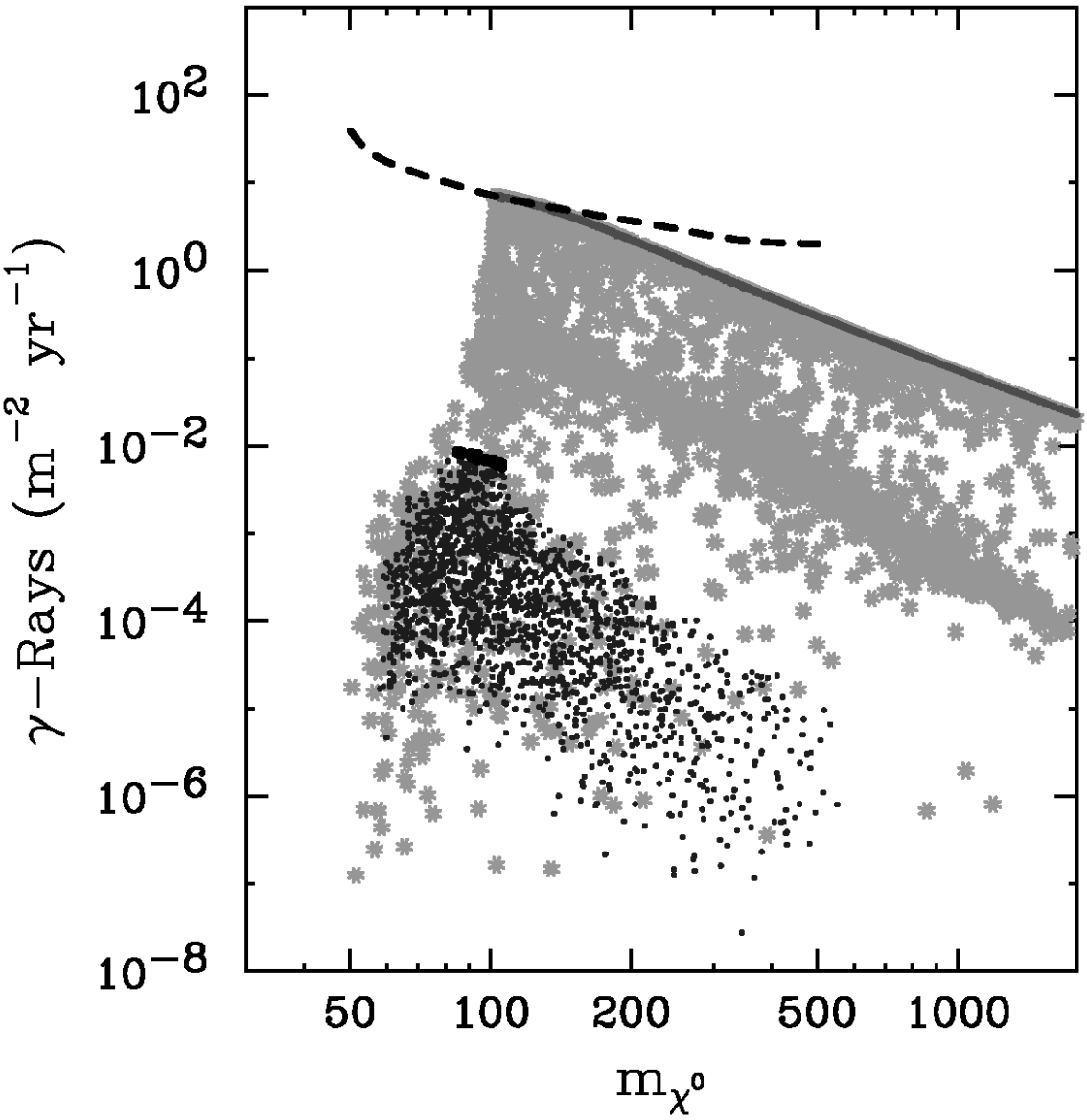

FIG. 9. The rate of gamma-rays from the process $\chi^0\chi^0 \to \gamma Z$ per square meter, per year of exposure, from the galactic center, verses neutralino mass. A smooth NFW halo profile is assumed. If a Moore, *et. al.* model were considered, each point would produce approximately a factor of 10^3 more events. As in figures 1 and 2, the lightly shaded region is for the general or phenomenological MSSM, the darker region corresponds to mSUGRA models, the shaded line represents AMSB models (minimal and non-minimal) and black circles indicate gaugino mediated models. For each point shown, the relic density is below the maximum value allowed by the WMAP data ($\Omega_\chi h^2 \leq 0.129$). Models that violate accelerator limits are also not shown, except for b to $s\gamma$ limits which will be discussed later. See the text for more details. Also shown is predicted sensitivity for the future experiment GLAST (dashed) [15]. In AMSB scenarios, the mass parameters M_1 and M_2 are proportional to their respective couplings, so the neutralino mass and annihilation cross section become correlated, leading to the single line across the figure.

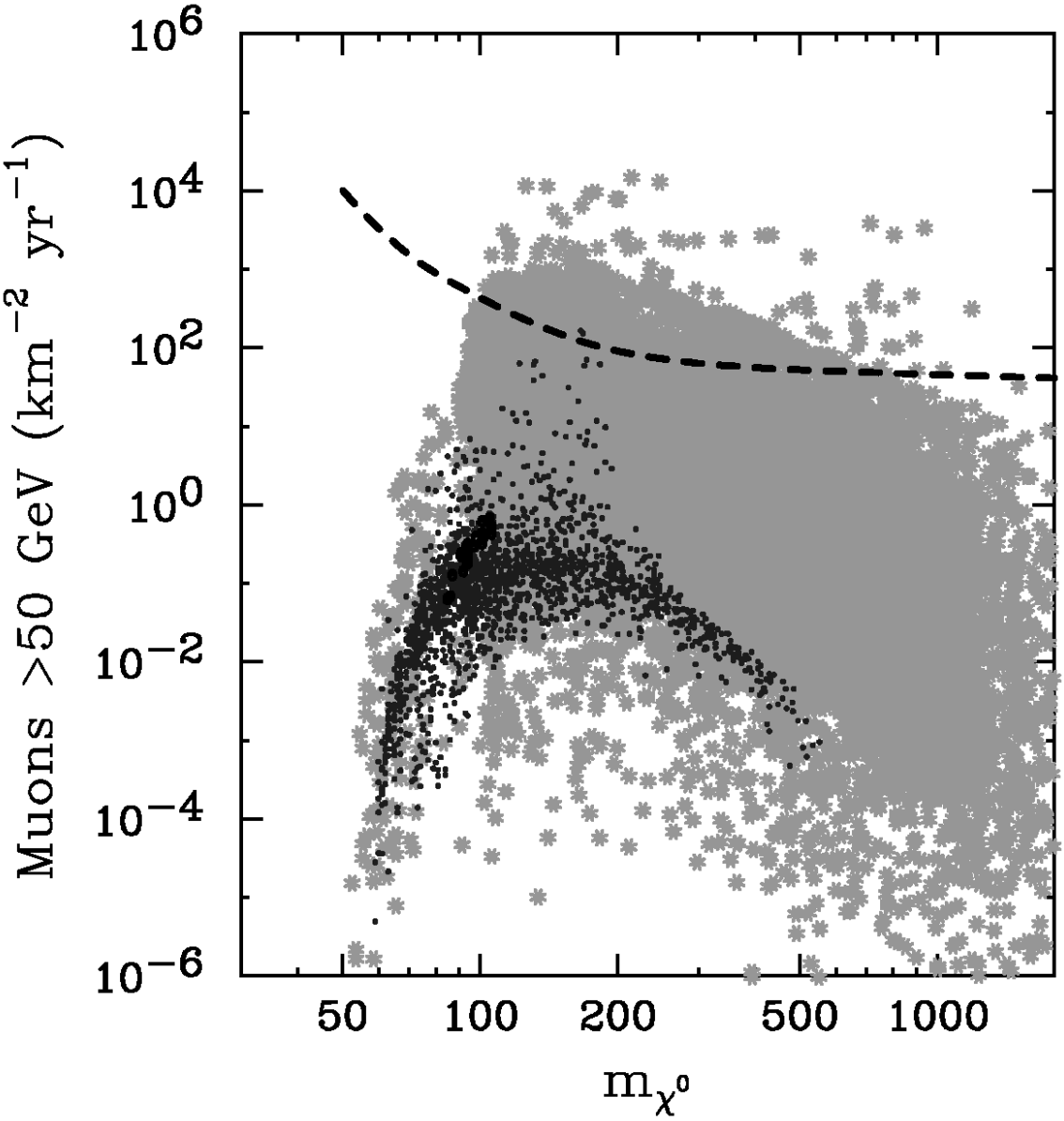

FIG. 10. The rate of muons (from charged current muon neutrino interactions) above 50 GeV per square kilometer, per year, from neutralino annihilation in the sun, verses neutralino mass. As in figure 1, the lightly shaded region represents the general or phenomenological MSSM, the darker region corresponds to mSUGRA models and black circles indicate gaugino mediated models. For each point shown, the relic density is below the maximum value allowed by the WMAP data ($\Omega_\chi h^2 \leq 0.129$). Models that violate accelerator limits are also not shown, except for b to $s\gamma$ limits which will be discussed later. See the text for more details. Also shown is the predicted sensitivity for the next generation neutrino telescope IceCube (dashed) [68].

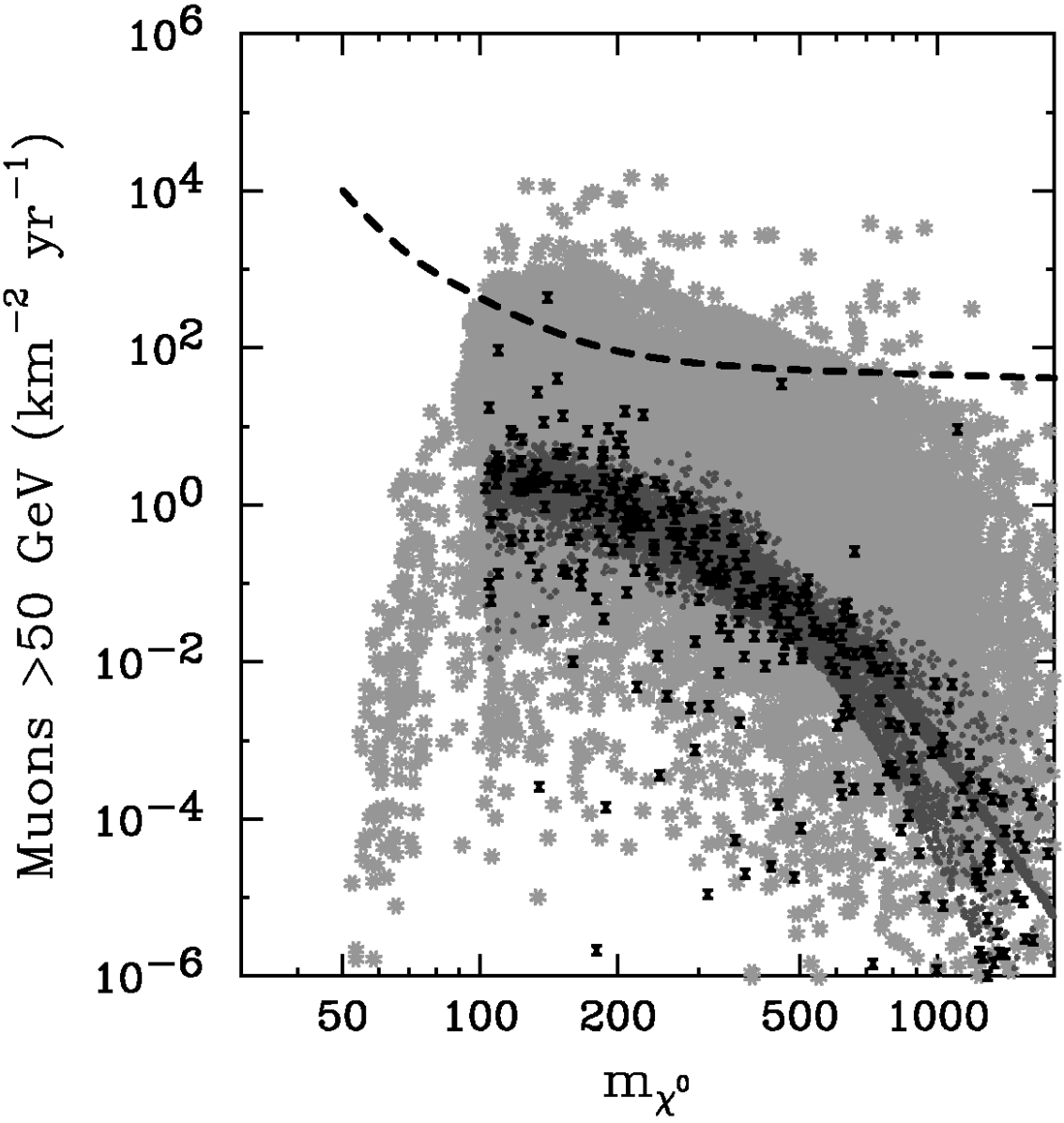

FIG. 11. The rate of muons (from charged current muon neutrino interactions) above 50 GeV per square kilometer, per year, from neutralino annihilation in the sun, verses neutralino mass. As in figure 2, the lightly shaded region is for the general or phenomenological MSSM, the darker shaded region show those models limited to minimal Anomaly Mediated Supersymmetry Breaking (mAMSB) models. Also shown are black X's which represent non-minimal AMSB models. For each point shown, the relic density is below the maximum value allowed by the WMAP data ($\Omega_\chi h^2 \leq 0.129$). Models that violate accelerator limits are also not shown, except for b to $s\gamma$ limits which will be discussed later. See the text for more details. Also shown is the predicted sensitivity for the next generation neutrino telescope IceCube (dashed) [68].

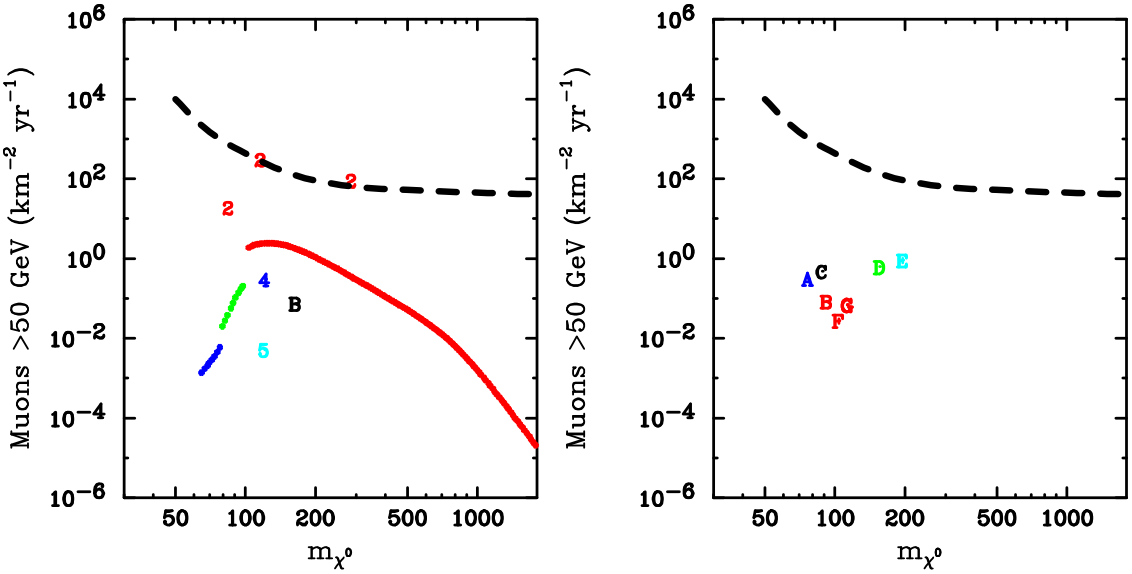

FIG. 12. The rate of muons (from charged current muon neutrino interactions) above 50 GeV per square kilometer, per year, from neutralino annihilation in the sun, verses neutralino mass. In the left frame, Snowmass slopes 1a, 3 and 9 and shown as lines from left to right, respectively. Snowmass points 1b, and samples of 2, 4 and 5 are shown as B, 2, 4 and 5 in the figure. In the right frame, each point corresponds to a theoretical prediction for a specific Michigan benchmark model. Models A through G are shown. See the text for more details. Along the length of each Snowmass slope shown, the relic density is below the maximum value allowed by the WMAP data ($\Omega_\chi h^2 \leq 0.129$). However, some of the points (rather than slopes) shown produce a larger relic density. Also shown is the predicted sensitivity for the next generation neutrino telescope IceCube (dashed) [68].

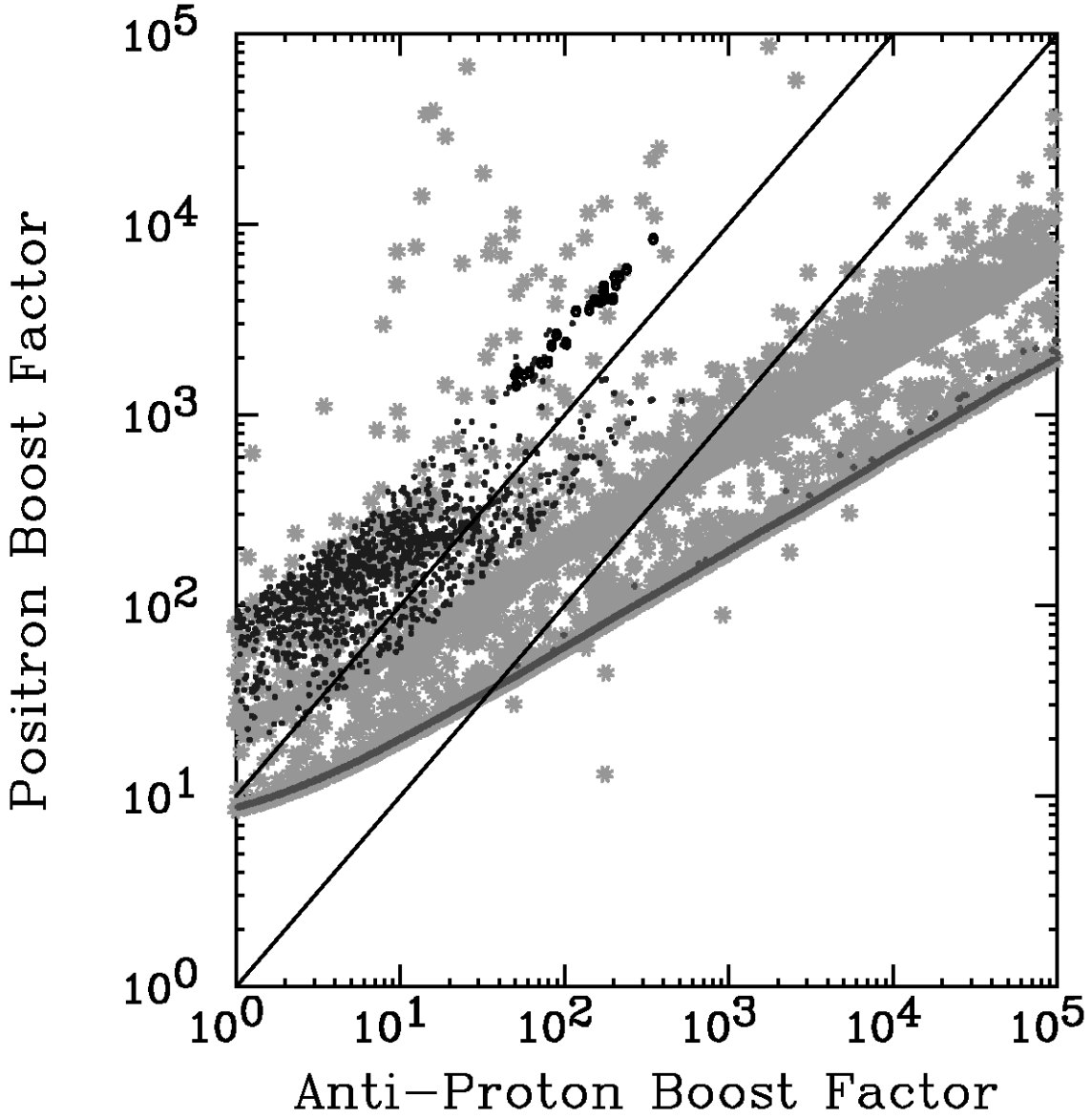

FIG. 13. The positron boost factor required to explain the HEAT positron excess [45,46] versus the maximum anti-proton boost factor consistent with the BESS anti-proton cosmic ray measurement [47]. As in figures 1 and 2, the lightly shaded region is for the general or phenomenological MSSM, the darker region corresponds to mSUGRA models, the shaded line corresponds to AMSB models (minimal and non-minimal) and black circles indicate gaugino mediated models. For each point shown, the relic density is below the maximum value allowed by the WMAP data ($\Omega_\chi h^2 \leq 0.129$). Models that violate accelerator limits are also not shown, except for b to $s\gamma$ limits which will be discussed later. See the text for more details. Solid lines correspond to the case when the positron boost factor is equal to the maximum anti-proton boost factor and for the case when the positron boost factor ten times larger than the maximum anti-proton boost factor. See the text for further discussion.

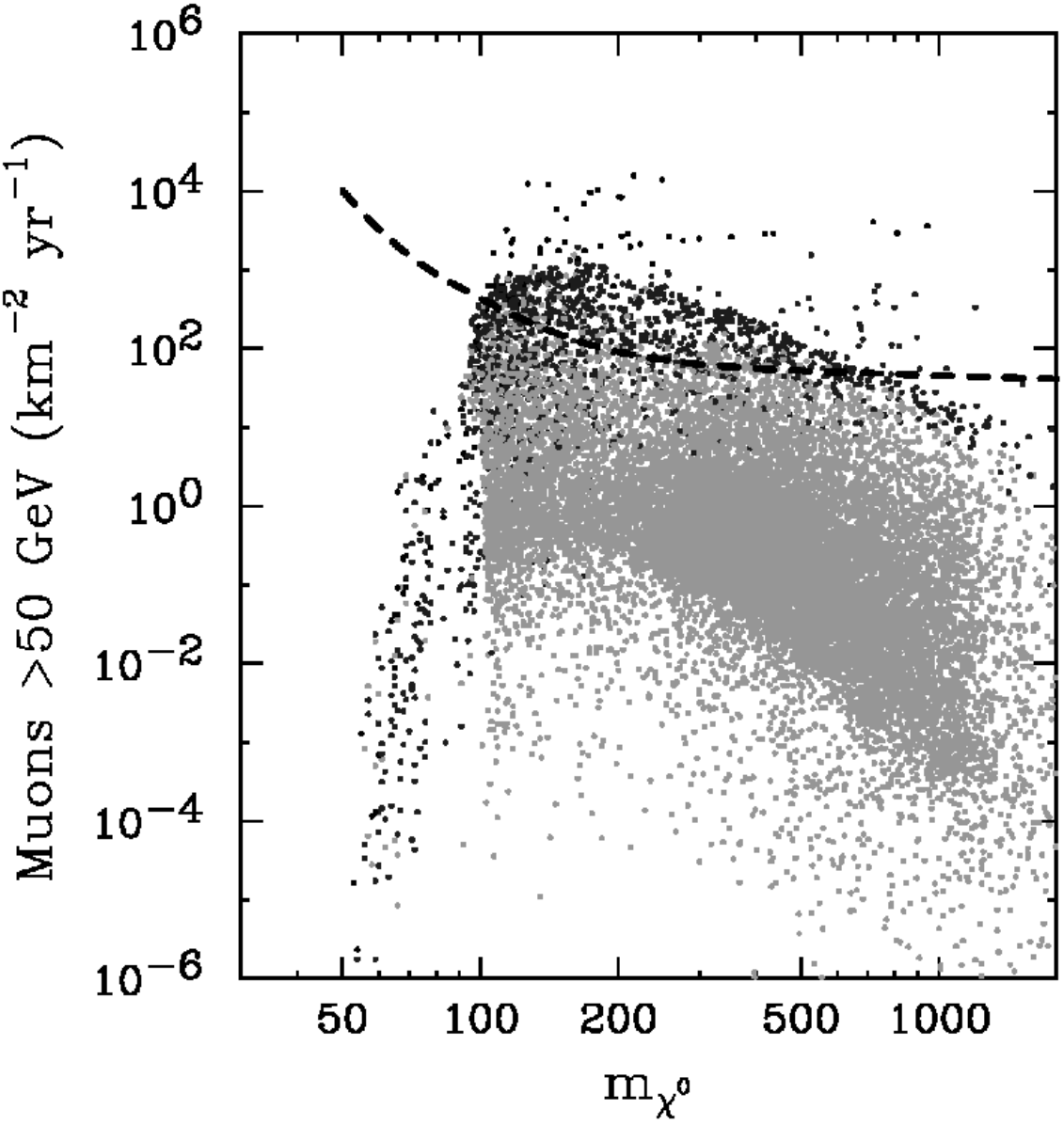

FIG. 14. The rate of muons (from charged current muon neutrino interactions) above 50 GeV per square kilometer, per year, from neutralino annihilation in the sun, verses neutralino mass. All models show were randomly selected from the general or phenomenological MSSM, as described in the text. Black X's represent models which have allready been excluded by current experiments such as CDMS-March 2002 [22], ZEPLIN 1-final 2002 [23] and Edelweiss-2000+2002 [24]. Darker points represent those models which can be tested by planned experiments with a sensitivity near that of the ZEPLIN 4-projection [29]. Lighter points fall below this sensitivity. Also shown is the predicted sensitivity for the next generation neutrino telescope IceCube (dashed) [68]. For each point shown, the relic density is below the maximum value allowed by the WMAP data ($\Omega_\chi h^2 \leq 0.129$). Models that violate accelerator limits are also not shown, except for b to $s\gamma$ limits which will be discussed later. See the text for more details.

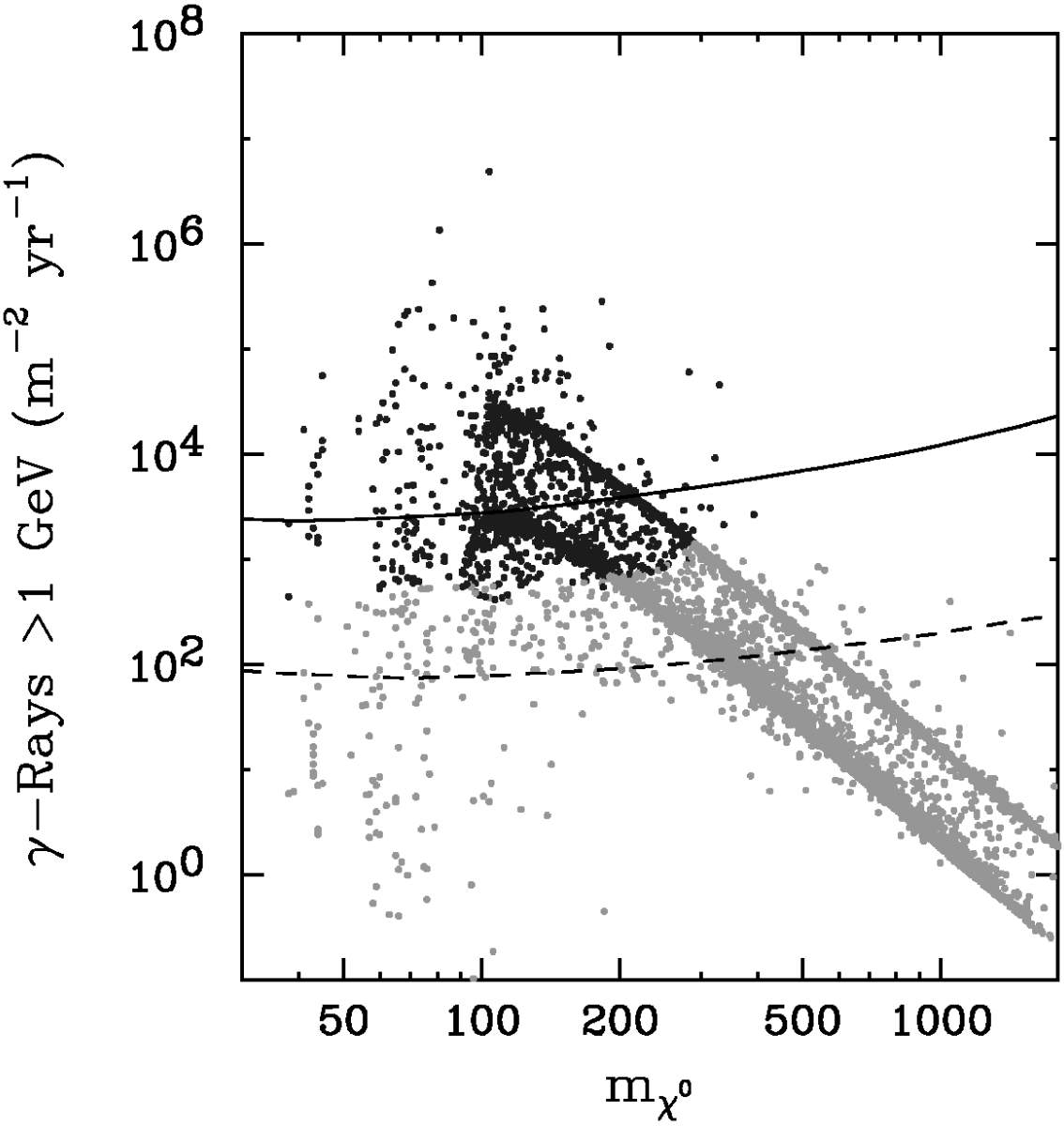

FIG. 15. The rate of continuum gamma-rays above 1 GeV per square meter, per year of exposure, from the galactic center, verses neutralino mass. A smooth NFW halo profile is assumed. If a Moore, *et. al.* model were considered, each point would produce approximately a factor of 10^3 more events. Models in the lightly shaded region do not overproduce anti-protons in the case of a smooth halo profile, as measured with the BESS experiment [47]. Models in the darker region, however, require some degree of fine tuning in the halo model, i.e. placing clumps at large distances, to accomodate this limit. Each model shown corresponds to a point in the general or phenomenological MSSM, as described in the text. For each point shown, the relic density is below the maximum value allowed by the WMAP data ($\Omega_\chi h^2 \leq 0.129$). Models that violate accelerator limits are also not shown, except for b to $s\gamma$ limits. See the text for more details. Also shown are limits from EGRET (solid) and predicted sensitivity for the future experiment GLAST (dashed) [14]. Note that those models in which EGRET is sensitive, anti-proton measurements appear to disfavor.

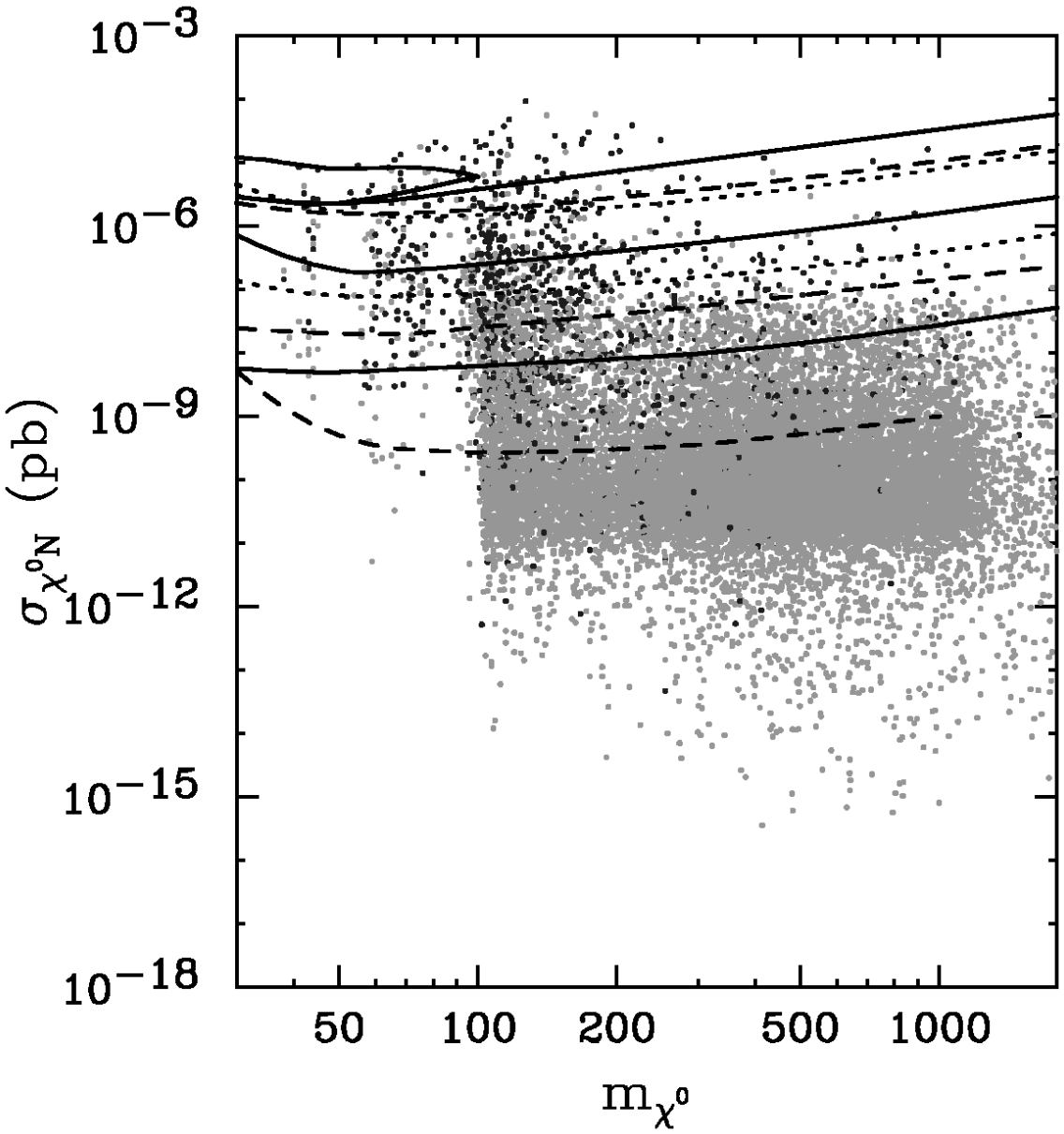

FIG. 16. The impact of the $b \to s\gamma$ constraint [64] on direct detection for models in the general or phenomenological MSSM. Lighter points are models which do not violate this constraint. Darker points do violate this constraint. Also shown are various experimental limits and sensitivities as in figures 1 and 2. See the text for more details.

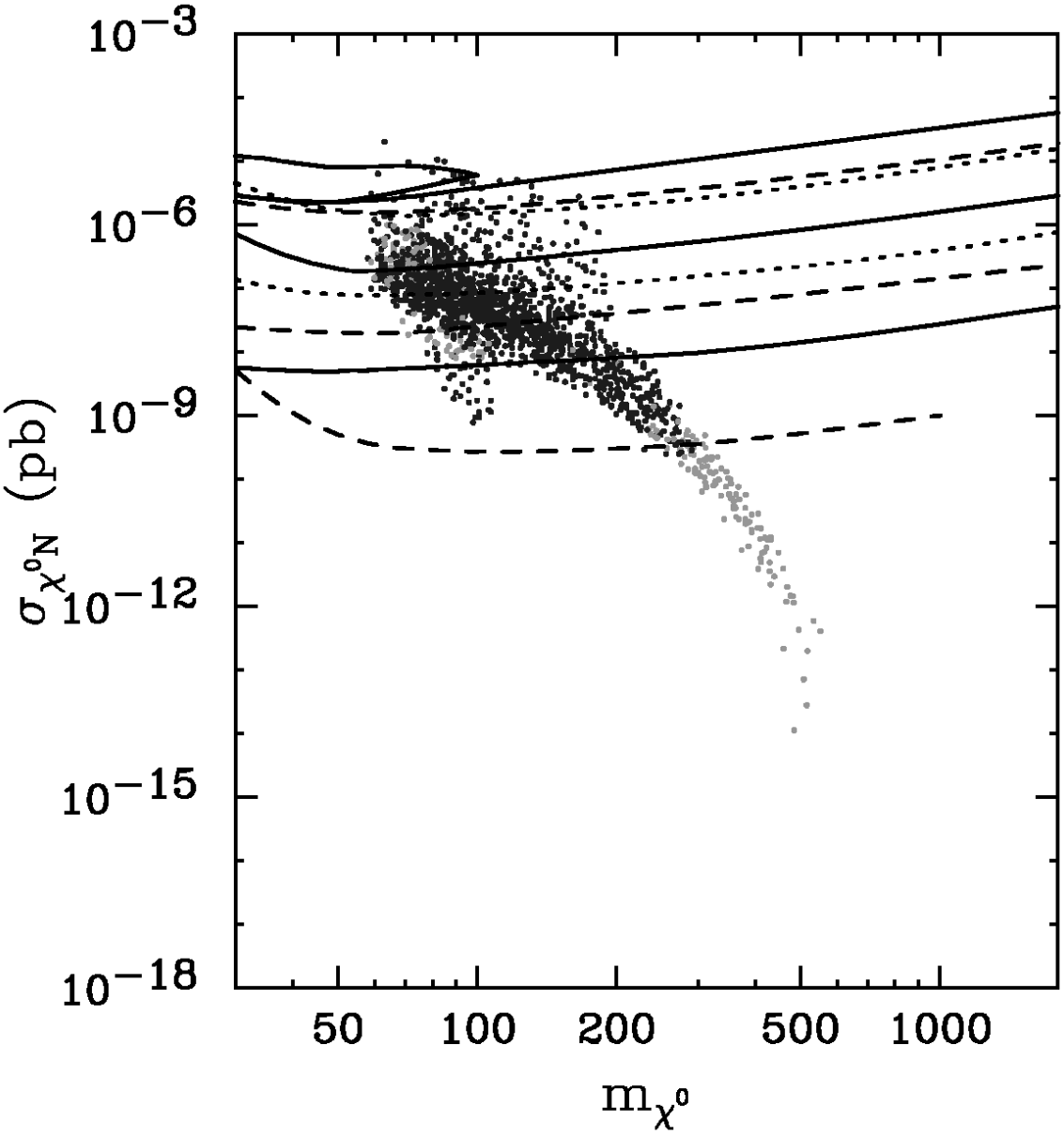

FIG. 17. The impact of the $b \to s\gamma$ constraint [64] on direct detection for models in the mSUGRA scenario. Lighter points are models which do not violate this constraint. Darker points do violate this constraint. Note that the small cluster of lighter points near 60-100 GeV and 10^{-8} pb are those mSUGRA points which we consider gaugino mediated ($m_{\tilde{f}}^2 \sim M_\lambda^2/(16\pi^2)$). Also shown are various experimental limits and sensitivities as in figures 1 and 2. See the text for more details.